School of Engineering and Mathematical Sciences

Aeronautical Engineering MEng 3/4

AE3030 Individual Project

Dissertation Report

An Experimental Study of Flow Separation on a Forward Facing Step using PIV Measurements

Supervisor:

Dr. Zhengzhong Sun

Prepared by:

Filip Livancic

London

Date: 01/06/2017

Table of Contents

1. Abstract

Effects of flow separation on a Forward Facing Step (FFS) are investigated to provide insights and highlight relationships affecting the characteristics of separation. Data collected from a wide array of step heights and Reynolds numbers illustrate factors affecting reattachment length and separation lengths of the recirculation region. A design of the Forward Facing Step has been manufactured for wind tunnel testing to investigate flow separation using Particle Image Velocimetry.

2. Introduction

The Forward Facing Step is geometrical approximation of mechanical devices such as cars, trucks or even segments of aerodynamic devices. The shape generates an adverse pressure gradient resisting the oncoming flow from the freestream. PIV measurements were collected from wind tunnel experiments on the Forward Facing Step to study the flow field. Analysis of the data illustrated the behavior of the Turbulent Boundary Layer (TBL) immersing the Forward Facing Step. Two separation regions are generated as a result of the adverse pressure gradient. The first region forms immediately at the foot and the other at the tip of the step extending downstream. Within the recirculation region exists a very low momentum flow in which there is no mass exchange with the free stream. The flow simply recirculates around itself which is being driven by the shear layer. The shear layer is the interface between the freestream and the recirculation region and is inherently turbulent as the flow separation at the tip of the step causes the flow to destabilize. The sizes of the separation bubble mainly depend on two factors: the ratio of the boundary layer thickness to the step height and the Reynolds number. Moreover, there is a strong link between the strength of the shear layer and the separation area of the bubble. Tall steps (in relation to the boundary layer) produce more extreme adverse pressure gradients, producing larger separation regions. The distribution of reattachment lengths are more negatively skewed downstream for the tall steps in comparison to the short steps because it takes longer for the boundary layer to re-energize itself to overcome the inertial forces. Furthermore the position of the reattachment point of the flow has tendency to fluctuate because of the undulations within the shear layer. The oscillating shear layer suggests that there vortex shedding due to local acceleration at the shear layer. The flow reattachment has a high level of surface pressure fluctuations and is likely a source of noise generation for FFS shaped devices.

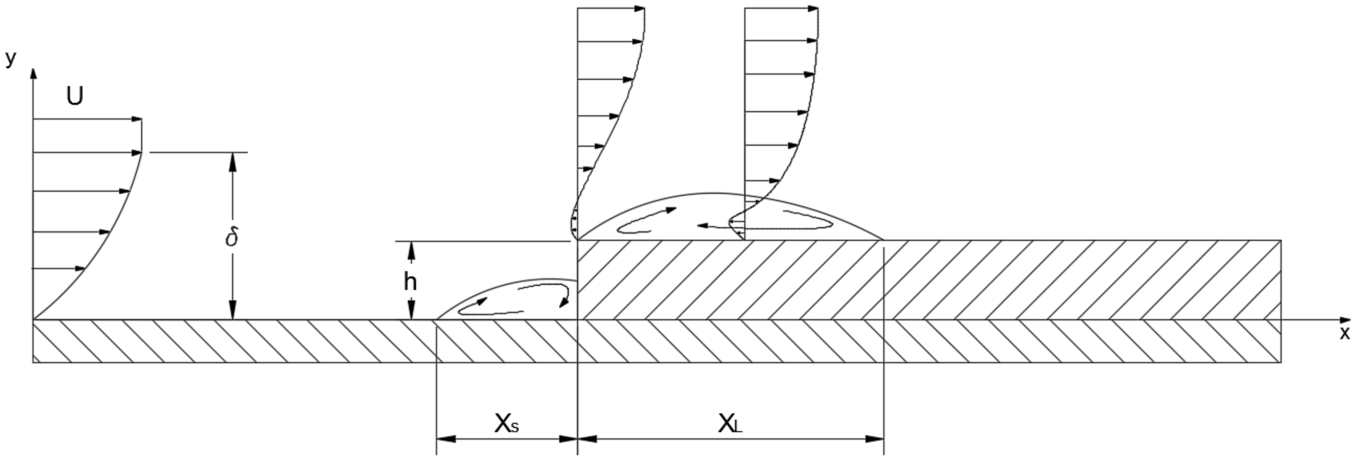

Figure(1): Schematic illustrating separation effects as boundary layer approaches step

3. Literature Review

3.1. Basic Flow Separation Characteristics

Two separation regions are present in a flow approaching a step. The first separation occurs at the foot of the step because of the adverse pressure gradient generated by the step. There is an upwash causing the flow to be forced upwards reattaching itself onto the face of the step. The flow immediately separates at the tip of the step and the recirculation region extends downstream. The recirculation region is larger downstream due to the low momentum flow being swept up by the higher velocity free stream and the presence of a favourable pressure gradient. Two main factors dictate how far the recirculation extends: The size of the boundary layer thickness δ in relation to the size of the step height h and also the Reynolds Number.

Depending on the ratio of $\frac{\delta}{h}$, the characteristics of the flow will change:

> $\frac{\delta}{h} \gg 1$: Flow behaviour almost acts as if there is an absence of a step, flow occasionally generates some eddies. But for the most part, very little resistance in the flow. Freestream turbulence however affects the reattachment length.
>
> $\frac{\delta}{h} > 1$: Low degree of flow separation because of weak adverse pressure gradient. Step comes into contact with a lower velocity component of the boundary layer. The reattachment position of the flow downstream depends strongly on the Reynolds number.
>
> $\frac{\delta}{h} < 1$: Higher degree of flow separation, stronger adverse pressure gradient. The step comes into contact with the free stream velocity of flow. Greater recirculation. Reattachment length is longer. Altering the Reynolds numbers has less effect on reattachment length when step is taller than the boundary layer thickness.

When the boundary layer is thicker than the height of the step, the Reynolds number greatly affects the reattachment length of the flow. A higher Re leads to longer reattachments and vice versa. Inertial forces begin to dominate the viscous forces. The turbulence between the boundary layer and freestream (also known as the shear layer) promotes an earlier reattachment since the boundary layer is more re-energised to overcome the viscous forces.

There is a strong correlation between the separation area (recirculation region) and the vorticity intensity downstream of the step. The intensity of the vortices are likely also dependant on the size of the step. If there was a large step, it would cause a large deceleration in the flow field. The low momentum flow in the boundary layer would be more likely to transition into a turbulent state and would mix with the flow within the shear layer. This effect would also be exaggerated if the Reynolds number of the flow was increased. Increasing the adverse pressure gradient, would increase the vorticity and increase the size of the recirculation region.

The reattachment position is not constant as there are low frequency oscillations in the flow field. This is because the shear layer is turbulent in nature. The undulations in the shear layer suggest that the reattachment point will fluctuate according to the instantaneous velocities and pressures in the flow. The surface pressures should also fluctuate because of the vortex shedding and local acceleration in the shear layer.

3.2. Statistical Analysis

Table (1) provides an overview of a range experiments concerning the flow separation over the Forward Facing Step. The table displays the separation lengths of the fore and aft recirculation regions for the respective step geometries and Reynolds numbers. Extensive data has been collected for region atop of the FFS, however there is very limited data concerning the separation lengths in front of the step.

Study	δ/h	h/δ	Re_h	X_L (h)	X_S (h)	$X_L\delta/h$	$X_S\delta/h$
M. Ji and M. Wang (2012)	0.01	120.5	405		-1.9	0.00	-225.3
	0.03	30.3	1620		-2.0	0.00	-59.4
	0.13	7.7	6480	2.2	-1.6	16.62	-12.1
Largeau and Moriniere (2007) [min]	0.30	3.3	28800	3.5		11.67	
Largeau and Moriniere (2007) [max]	0.30	3.3	128200	5.0		16.67	
M. Awasthi (2012)	0.40	2.5	106000	4.1		10.28	
	0.40	2.5	213000	4.2		10.53	
Bergeles and Athanassiadis (1983)	0.48	2.1	27000	3.8		7.81	
E. Fiorentini et al. [min]	0.50	2.0	4400	2.0		4.00	
E. Fiorentini et al. [max]	0.50	2.0	26300	3.0		6.00	
M. Ji and M. Wang (2012)	0.53	1.9	25920	2.9	-0.9	5.53	-1.6
Moss and Baker (1980)	0.70	1.4	50000	4.7		6.71	
Gasset et al. (2005)	0.70	1.4	50000	5.0		7.14	
Zhang (1994)	0.70	1.4		4.0		5.74	
Lerclercq et al. (2001)	0.70	1.4	17000	3.2		4.57	
M. Awasthi (2012)	0.85	1.2	26600	3.6		4.24	
	0.85	1.2	53200	3.8		4.48	
Weijie Shao (2014)	0.88	1.1	1600	1.7		1.89	
Sherry et al. (2009) [min]	0.90	1.1	2000	1.1		1.22	
M. Awasthi (2012)	0.96	1.0	6640	1.6	-1.5	1.66	-1.6
	0.96	1.0	13300	3.2		3.33	
D S Pearson et al. (2011)	1.63	0.6	20500	2.5		1.53	
Weijie Shao (2014)	1.90	0.5	3200	1.8		0.96	
Arie et al. (1975)	1.96	0.5		2.5		1.28	
Farrabee and Casarella (1986)	2.40	0.4	21000	3.0	-1.9	1.25	-0.8
Sherry et al. (2009) [max]	4.00	0.3	20000	4.0		1.00	
Weijie Shao (2014)	4.68	0.2	4800	2.3		0.48	
Camussi et al. (2008) [min]	5.00	0.2	8800	1.5	-1.9	0.30	-0.4
Camussi et al. (2008) [max]	5.00	0.2	26300	2.1		0.42	
Castro and Dianat (1983)	5.20	0.2	50000	1.4	-1.5	0.27	-0.3
Agelinchaab and Tachie (2008)	9.30	0.1	19200	4.1	-1.7	0.44	-0.2

Table (1): *Historical Data of Forward Facing Step*

Figures (2) and (3) highlights the distribution of data of reattachment lengths on the top of the step based on other FFS experiments in varying different step heights and different Reynolds numbers. X_L and X_S are measured in step height and the datum is taken from the face of the step.

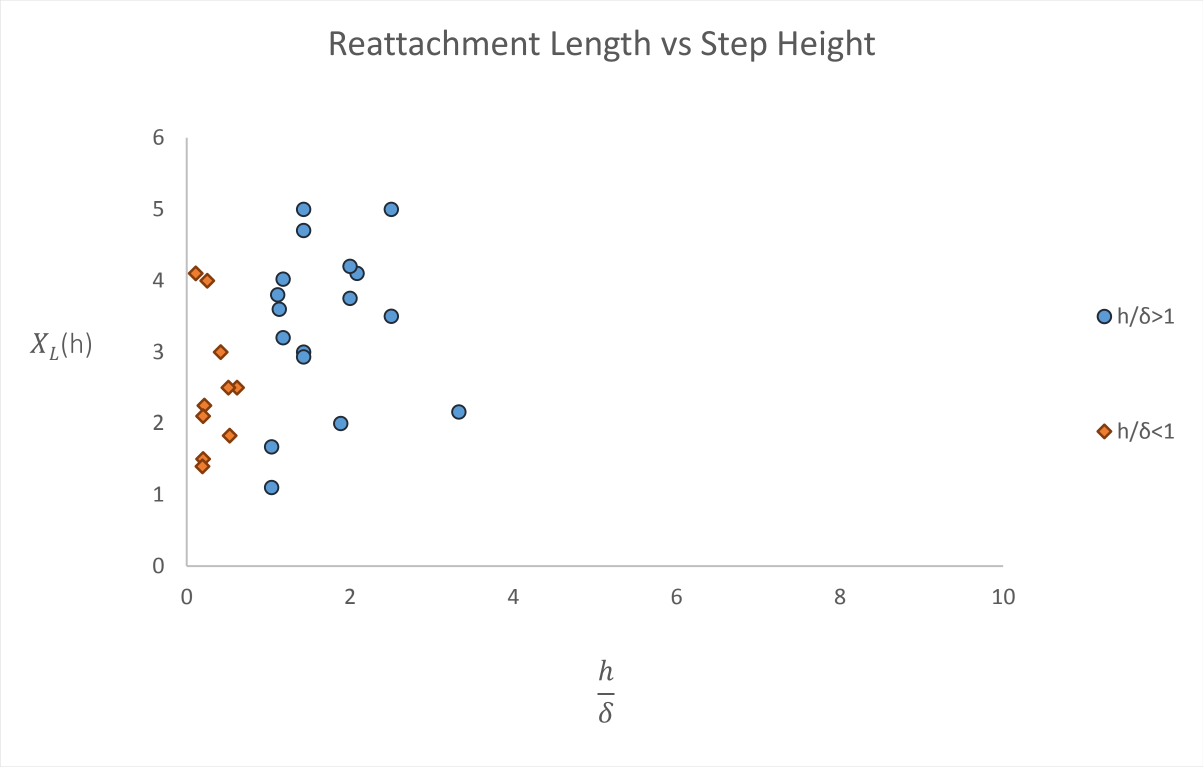

Figure (2): Graph illustrating distribution of reattachment lengths of downstream separation bubble based on step height

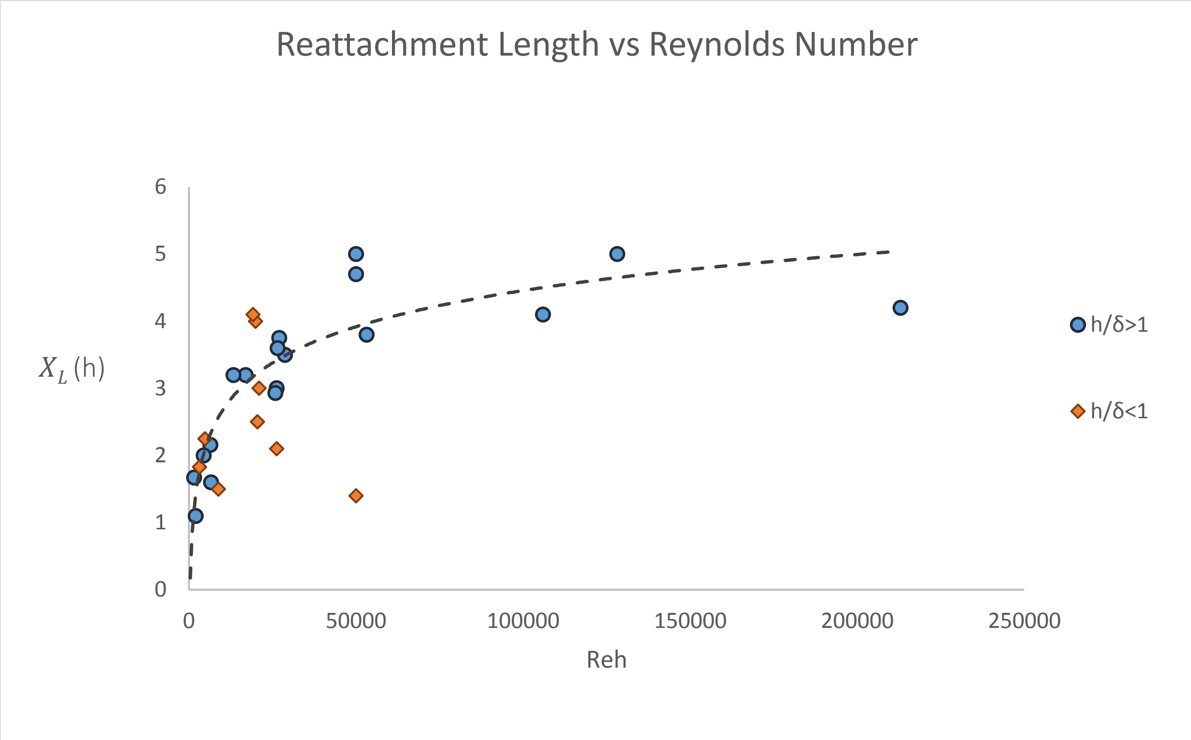

Figure (3): Illustrating distribution of reattachment length based on Reynolds number at the given step height

For all step heights smaller than the boundary layer thickness (h/δ <1), the distribution of the reattachment points on the step vary in a range of distances varying from 1-4h as shown in Figure (2). The flow does not reattach before 1h because of the low momentum of the flow being dominated by the inertia. It takes at least 1 step height for the boundary layer to re-energize itself after being tripped up by the step. There seems to be a higher density distribution of reattachments before 3h, which seems to be characteristic of smaller steps. However the step height is not the only primary cause affecting reattachments as X_L it is also dependant on the Reynolds number of the flow. The Reynolds number fluid over the step is a considerable factor. Higher velocity flows mean that the boundary layer travels further when gathering kinetic energy to overcome the adverse pressure gradient. The small step height creates small separation bubbles which is why the reattachments are generally shorter. It can be seen in Figure (3) that an increase in the Re_h, has a slight effect in extending the reattachment length. The separation bubble is expected to have a high aspect ratio in comparison to bubbles produced from the tall steps.

For the steps taller than the boundary layer (h/δ>1), there is a higher density of reattachment lengths beyond 3h. Large steps produce large disturbances to the flow field, resulting in larger separation bubbles. The tall step creates a larger adverse pressure gradient, stagnating the flow to a greater degree. Thus the overall dimension of the separation region scaled up slightly. The bubble has a smaller aspect ratio compared to the smaller steps. The higher Reynolds numbers do not appear to have an extensive effect on the extension of the separation bubbles. The length of the recirculation region is less dependent on the Re_h when the geometry of the step is large. Increasing the Re beyond $5x10^4$ becomes ineffective with respect to extending the length of the separation region. The limit to X_L according to the data plateaus off at 5h for tall steps as illustrated in Figure (3) for (h/δ>1).

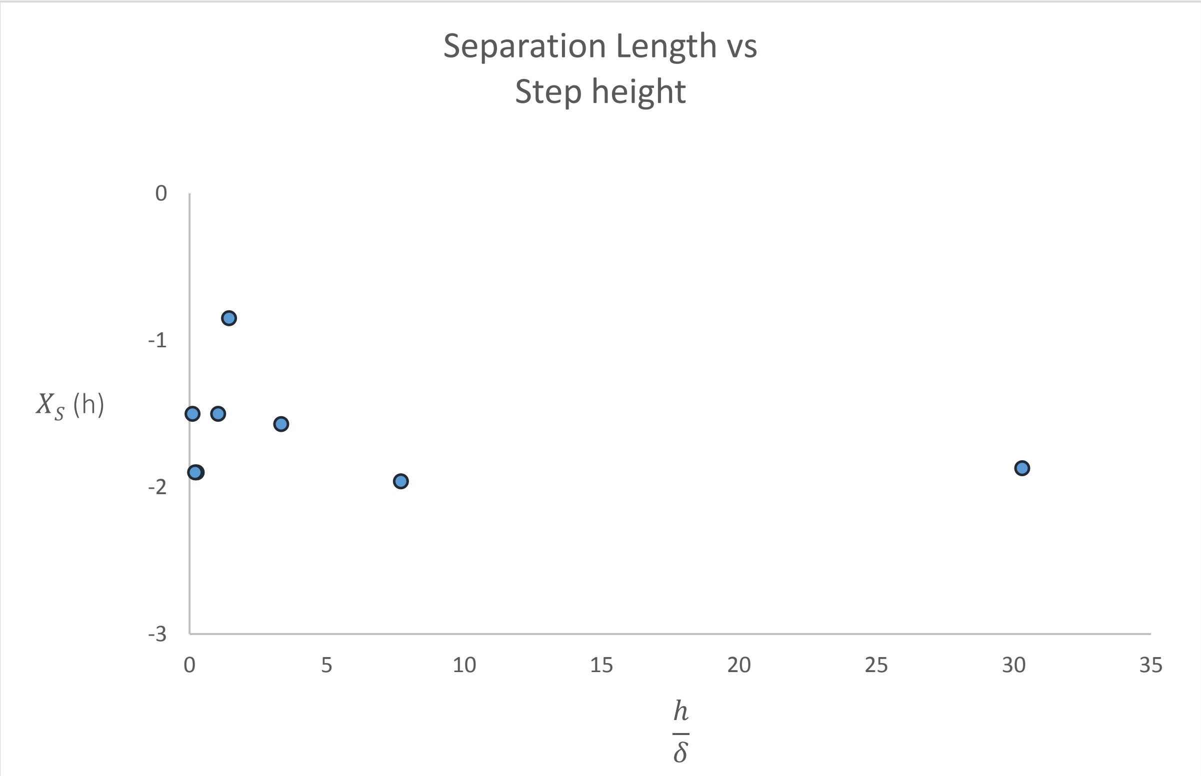

Figure (4): Distribution of separation length for various step heights of upstream separation bubble

Figure (4) shows the data distribution of the separation length of the foremost separation region being produced at the foot of the FFS. Unlike the separation region produced downstream on top of the step, the separation bubble at the foot is comparatively smaller. X_S is approximately less than half the size of the X_L on average. The step causes a stagnation of flow near the foot of the step, however since the dimension of the step is very small, then there is less space for the stagnant airflow to accumulate. In light of this, even when the step height is increased, the separation length doesn't grow any further. X_S plateaus at -2h for the greatest geometry whereas downstream the X_L plateaued at approximately 5h. The adverse pressure gradient seems to have lesser effect at the foremost region of flow separation.

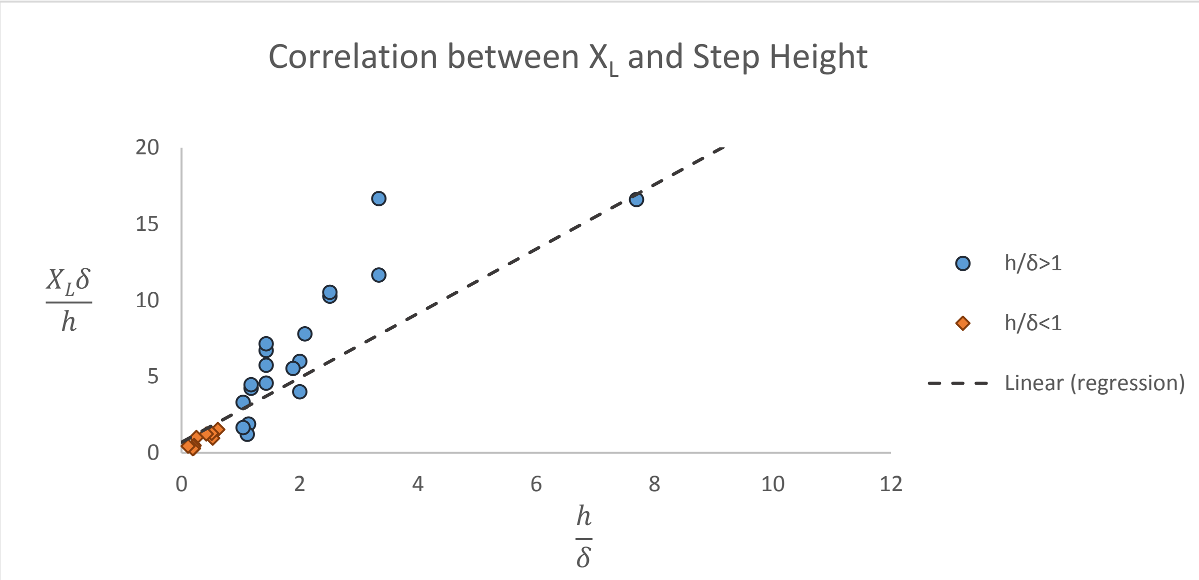

Figure (5): Graph illustrating the relationship between changes in geometry and the normalised reattachment length

Figure (5) shows the relationship between changes in geometry and the reattachment length of the separated flow on the step. The ratio of X_L to h/ δ to normalise the data and was plotted on the y-axis against h/ δ to see the geometrical effects on the X_L. There appears to be a significant correlation between these parameters. A linear regression was calculated as shown in Table (3) and it is shown that the value of r was equal to 0.88. This suggests a very high correlation between the step height and the reattachment length. Incremental increases in the step height will very likely extend the recirculation region at a small scale going downstream.

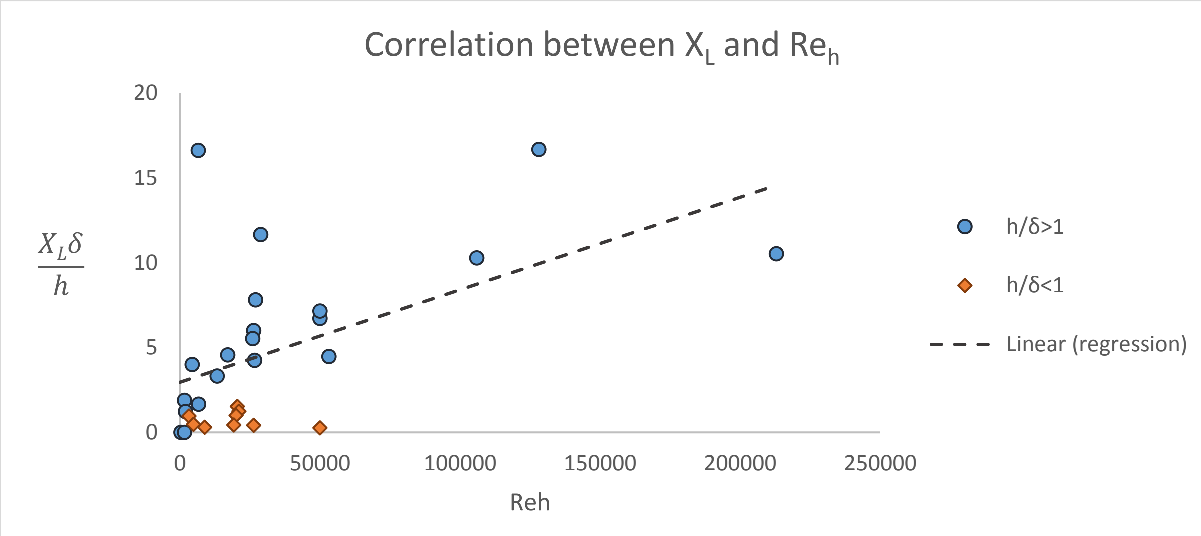

Figure (6): Graph illustrating the relationship between changes in geometry and the normalised reattachment length

In Figure (6), the Reynolds number showed slightly weaker correlation against the parameter $X_L\delta/h$. From the linear regression, the value of r was calculated to be 0.55 as documented in Table (2). Flow separation is more so dependent on the lower spectrum of Reynold Number values. As stated previously in Figure (3), the limit to which the extensions of X_L occur is at 5 step heights. The greater the geometry of the step, the less effective changes in the Reynolds Number affecting the reattachment length of the flow.

3.3. Flow Observations

The recirculation regions contain two types of vortices within the vortical structure. The vortices are either prograde (rotating clockwise) or retrograde (rotating anti-clockwise). The prograde vortices are predominantly located near the face of the step, particularly in the streamwise direction. "Retrograde vortices increase with wall-normal distance and then found to decrease further upwards" [7]. (S.I. Shah, pg. 2). There are hair pin vortices located in the wall turbulence. The hairpin vortex moves 45 degrees to the stream wise direction and it features counter rotating legs that are joined through a head segment and seems to be quasi-symmetric. The structure of the hair pin vortex is similar to that of the horseshoe vortex. Increasing the Reynolds number of the flow elongates the vortical structures causing the transition from horseshoe to hairpin. Therefore the aspect ratio of a hair pin vortex is much greater than the horseshoe vortex.

Near wall streaks become weak due to the presence of an adverse pressure gradient. The mean spacing of the streaks tended to increase further downstream of the flow since the effect of the adverse pressure gradient becomes more prevalent. The streaks indicates the onset of flow separation. Flow separation causes the streaks disappeared from existence. [7]. (S.I. Shah, pg. 2). The adverse pressure gradient has a damping effect on the vortical structures which increases the spacing of the vortical structures. Therefore this is the reason why large steps produce separation bubbles with a greater area. The stronger adverse pressure gradient increases the spacing of the vortices, thus creating a large recirculation region in which the vortices are occupying. Hairpin vortices tend to form in vast amounts near the wall surface of structures. Direct Numerical Simulations (DNS) of Lee and Sung (2008), (2010) of the coherent structures within a Turbulent Boundary Layer (TBL) found that in an adverse pressure gradient, there is a higher proportion of prograde vortices in relation to retrograde.

Generation of hairpin vortices are enhanced by the flow separation mechanism. The development of these newly created vortices near the wall in both the spanwise and streamwise direction of the wall normal planes. The near wall peak vortex densities coincides with the outward movement of the turbulence peak. (S.I. Shah, pg. 13). The mean vortex radius increases away from the wall normal direction in all directions and the spanwise vortices are bigger than the streamwise vortices. In the recirculation region, there is a higher density of vortices developed and the mean radius of these vortices are smaller compared to that of the outward flow.

Turbulent boundary layer (TBL) flow over a step produces greater pressure fluctuations in comparison to a smooth flat surface (Minsuk Ji et al. pg471) [8]. Since the step is scaled similar in size to the boundary layer, the associated unsteady pressure can induce structural vibrations as well as generate noise which radiates downstream. Farabee & Casarella (1984, 1986) investigated steps under 50% of the boundary layer thickness, the Reynolds numbers in the range of $2600 < Re < 6000$ produce pressure fluctuations at the reattachment point was found to be 5 to 10 times bigger in comparison to beneath equilibrium boundary layers (Minsuk Ji et al. pg472) [8]. The maximum p_{rms} value is located at the reattachment point of the flow. The peak value quickly decays beyond the reattachment point. However, the frequency spectra indicates that energized regions of spectra remain identifiable 36-72 step heights downstream. This suggests that the noise generated after passing over the step lingers downstream but likely at a lower magnitude. As the step height increases, the incremental increase of peak pressures decreases upstream. The vertical velocity component is closely related to the surface pressure fluctuations. Since the larger steps induce greater upwash velocities on the face of the step, there is likely going to be a stronger shear layer. The stronger shear layer will enhance the surface fluctuations on the surface of the step and therefore produce more noise.

In the middle of the separation bubble, pressure related sources convect more slowly than the boundary layer sources. In addition the surface pressure fluctuations in the reattachment region continue to be dominated by the convecting shear layer generated structures.

For smaller steps, the recirculation region in front of the face of the step is has a longer length and the boundary layer has to travel further towards the step. As the boundary layer passes over the separation bubble, there is a very mild acceleration over the bubble in comparison to a bubble with a short length. This corresponds to the lowest energy levels at higher frequencies. The bigger steps would show an increase in spectral levels caused by the enhanced turbulence in the shear layer. This would be a result of a stronger acceleration of the boundary layer over the separation bubble and this is likely to increase the strength of the flow with the separated shear layer. As the step height increases, the turbulence-turbulence interaction increase and become more pronounced. In addition the turbulent kinetic energies also increase.

Downstream at distances beyond 3h, the spectral levels are reduced in the case of most step sizes. Also, wherever the spectral levels begin to fall off, it is a symptom of vortex shedding at the shear layer. For steps producing a strong separated shear layer, a long distance is required for equilibrium to be restored to the flow because of the initial perturbations caused by the forward facing step.

4.1. Design Work

The design of the Forward Facing Step involved making a modification to an existing model of a wooden plate. The essence of the modification was to make it possible to view the airflow over the step and record the flow field using the PIV technique. A hole is cut into the wooden plate for the laser to provide illumination to the airflow so that recording can ensue. The hole had to be covered with a transparent surface both allowing the light to pass through as well as acting as a surface for the airflow to move along. Perspex was the material of choice to perform the task. A large step with a thickness of 10mm is screwed into the top of the wooden plate to perform as the Forward Facing Step. The step is positioned at the midpoint of the viewing window which is about 600mm downstream of the leading edge, provide ample opportunity for boundary layer development. The viewing section is large enough to study the upstream and downstream regions of the step. The largest recorded reattachment length is approximately 5h and the viewing window has a region 130mm in which the flow can be captured, more than enough to study the effects of flow separation. The step is also manufactured using Perspex, allowing the light to penetrate through the step, thus making it possible to study the flow downstream. Furthermore fashioning the step out of a single material reduces the complexity of the design and doesn't have significant drawbacks. More layers of Perspex can be layered and secured atop of the first step in order to modify the ratio of step height to boundary layer thickness.

However the flaw with the design is that the light intensity of the laser is reduced as it passes from each layer of Perspex. This is especially true is the experiment chosen to project the laser from beneath the model. An additional slit had to be cut into the bottom layer of Perspex to allow a greater light intensity and to reduce any systematic errors arising from the recording of the flow field using the PIV technique. This design revision doesn't create any issues since the flow is only being studied over the upper surface of the FFS. The model is very wide in relation to dimensions of the slit, so the turbulence produced from the slit will not interact with the flow field from the top surface. The camera is positioned facing near the upper surface of the Forward Facing Step. Thus only the particles in the flow field atop the wooden plate will be recorded. Additionally the model has a W/h (Width to height) ratio over 100 which is an accommodating part of the design such that the 3D effects are significantly negated as a result since the flow field being studied in a planar manner. The 3D effects emerging from edges of the plate help in not disturbing the flow being observed in the centre of the wooden plate.

Another challenge involved with doing this modification is that it is difficult to fashion wood to the correct tolerance. The wooden plate was made out of MDF and the surface of the wooden plate is particularly large, therefore it's not perfectly flat. This is especially problematic when trying to design the viewing section of the Forward Facing Step. The viewing window must be completely flush with the surface of the wooden plate. Any edges protruding from the surface could trip the boundary layer, causing the flow to transition into a turbulent state unintentionally and disturb the experimental results.

The solution to the problem was designing a double sided recess in the wooden plate in which the levelness of the Perspex window can be adjusted from beneath the model to match the wooden surface. A layer of Perspex is screwed into the bottom recess and a layer of Perspex is screwed into the top layer of the recess. The screw heads emerge from the bottom layer of Perspex. This is to prevent any imperfection which could interact with the flow on the top surface, and the surface is left flush. Only partial holes and threads are implanted to secure the upper layer of Perspex whilst leaving the surface untouched. The concept of the design introduces a push-pull screw mechanism. The innermost set of screws secure the layers to the wooden plate and have countersunk screw heads to improve the streamlining over the surface. The outer set of screws have partial threads and have a flat end and additionally these screws have pan heads so that a bit of clearance is available when making adjustments. The purpose of these screws are to provide leverage for jacking the edges of the top layer of Perspex upwards, making the edges flush with the wooden surface. These screws are not performing as fasteners in this design, only as adjusters. There is a small 1mm clearance for the top layer of Perspex to allow these adjustments to be made.

The parts, assemblies, drawings were produced on SolidWorks and are illustrated on the following pages. All dimensions are in mm and the scales apply for an A3 paper format.

Design Work

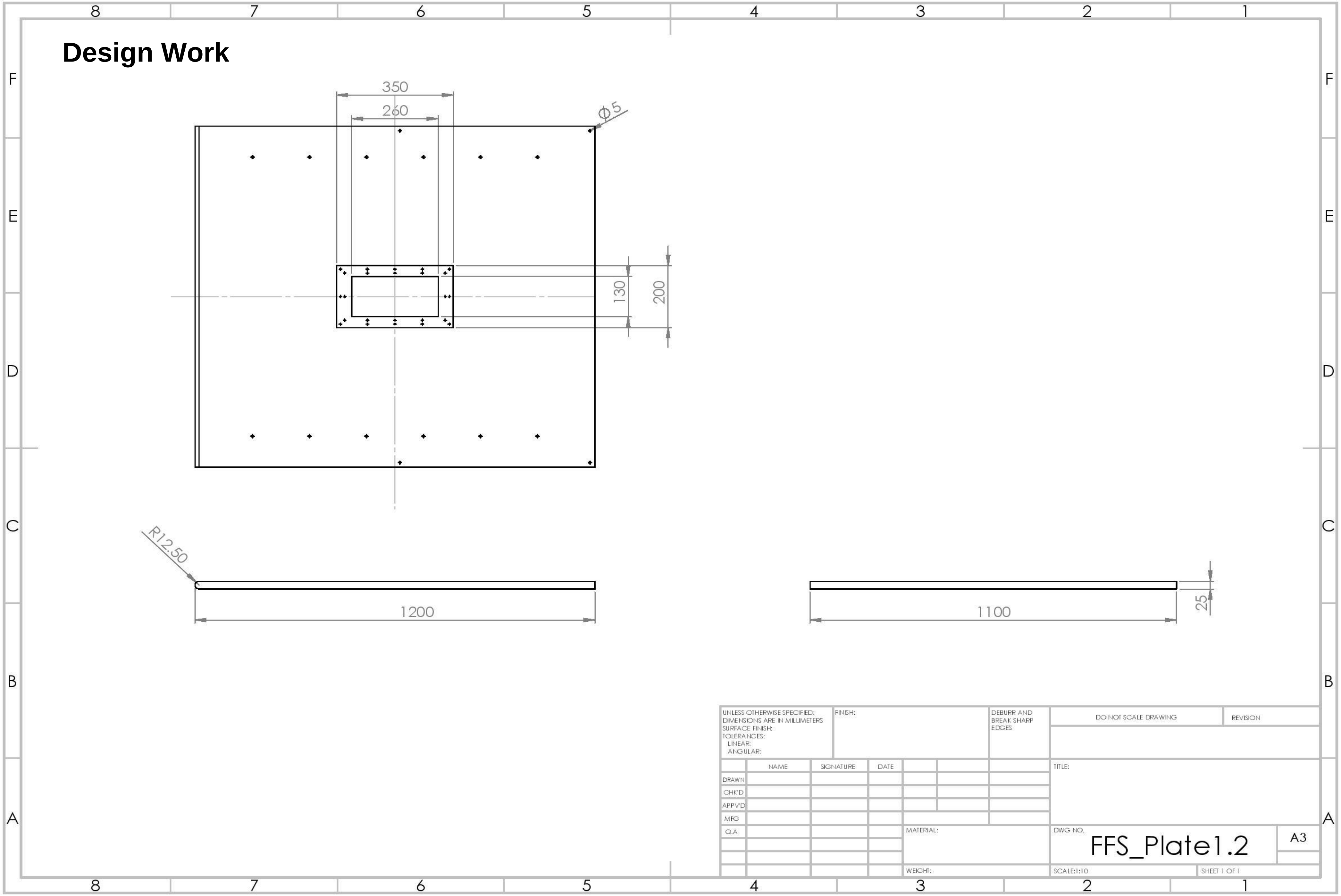

350
260
Ø5
130
200
R12.50
1200
1100
25
UNLESS OTHERWISE SPECIFIED:
DIMENSIONS ARE IN MILLIMETERS
SURFACE FINISH:
TOLERANCES:
LINEAR:
ANGULAR:
FINISH:
DEBURR AND BREAK SHARP EDGES
DO NOT SCALE DRAWING
REVISION
NAME
SIGNATURE
DATE
DRAWN
CHK'D
APPV'D
MFG
Q.A
TITLE:
MATERIAL:
DWG NO.
FFS_Plate1.2
A3
WEIGHT:
SCALE:1:10
SHEET 1 OF 1

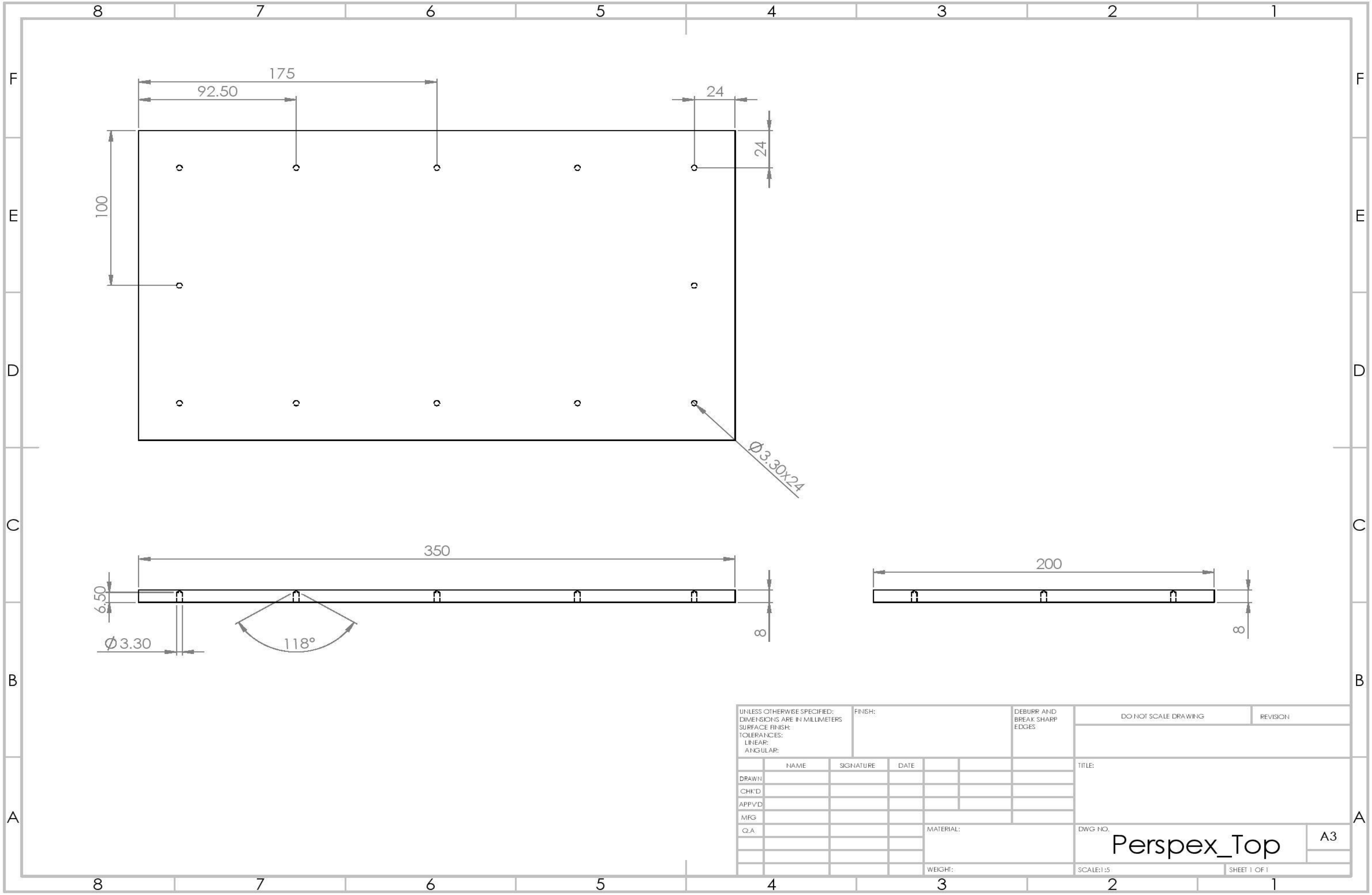
175
92.50
24
24
100
Ø3.30x24
350
6.50
Ø3.30
118°
8
200
8
UNLESS OTHERWISE SPECIFIED:
DIMENSIONS ARE IN MILLIMETERS
SURFACE FINISH:
TOLERANCES:
LINEAR:
ANGULAR:
FINISH:
DEBURR AND BREAK SHARP EDGES
DO NOT SCALE DRAWING
REVISION
NAME
SIGNATURE
DATE
DRAWN
CHK'D
APPV'D
MFG
Q.A
TITLE:
MATERIAL:
DWG NO.
Perspex_Top
A3
WEIGHT:
SCALE:1:5
SHEET 1 OF 1

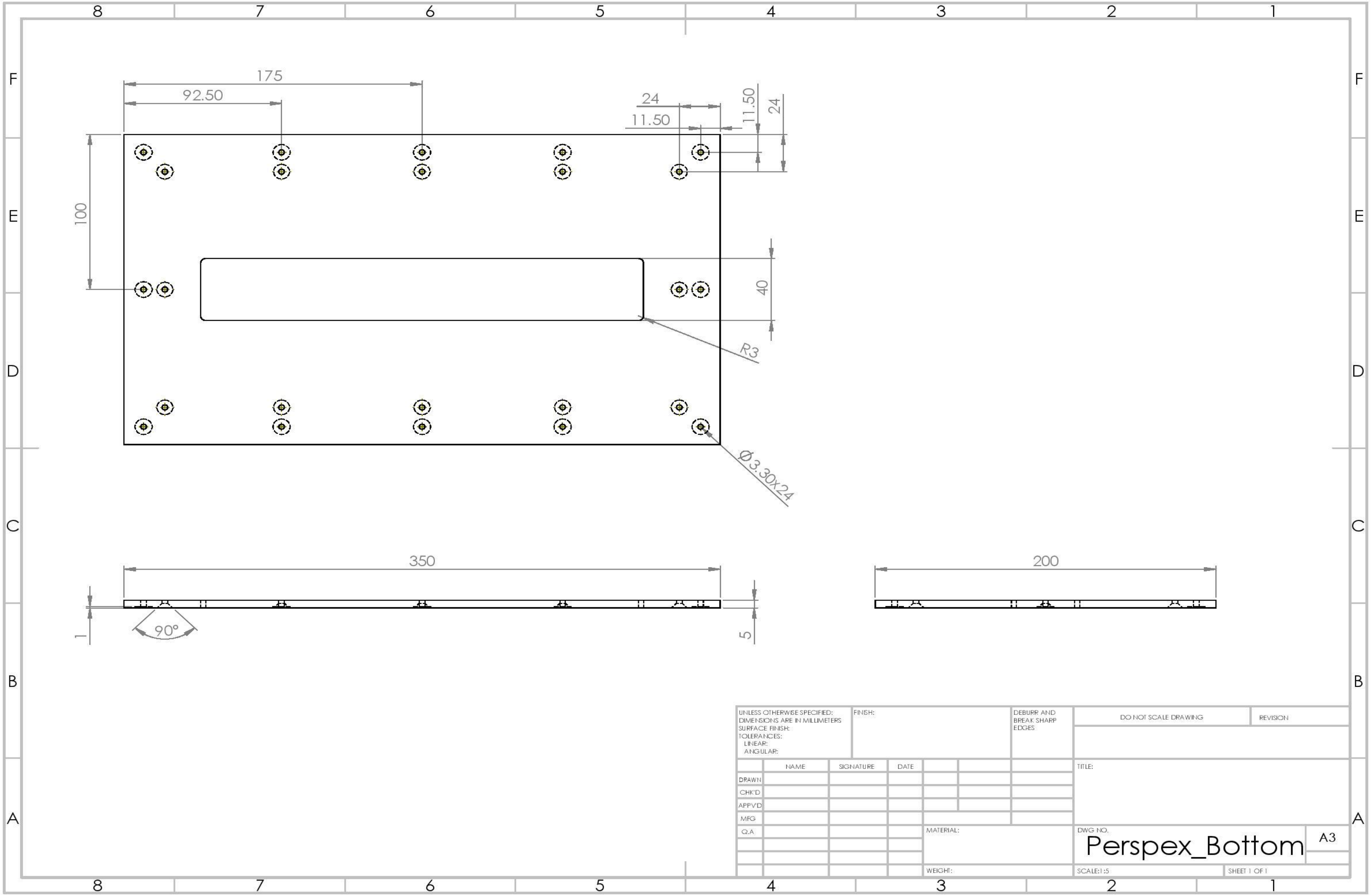
175
92.50
24
11.50
11.50
24
100
40
R3
Ø3.30x24
350
200
1
90°
5
UNLESS OTHERWISE SPECIFIED:
DIMENSIONS ARE IN MILLIMETERS
SURFACE FINISH:
TOLERANCES:
LINEAR:
ANGULAR:
FINISH:
DEBURR AND BREAK SHARP EDGES
DO NOT SCALE DRAWING
REVISION
NAME
SIGNATURE
DATE
DRAWN
CHK'D
APPV'D
MFG
Q.A
TITLE:
MATERIAL:
DWG NO.
Perspex_Bottom
A3
WEIGHT:
SCALE:1:5
SHEET 1 OF 1

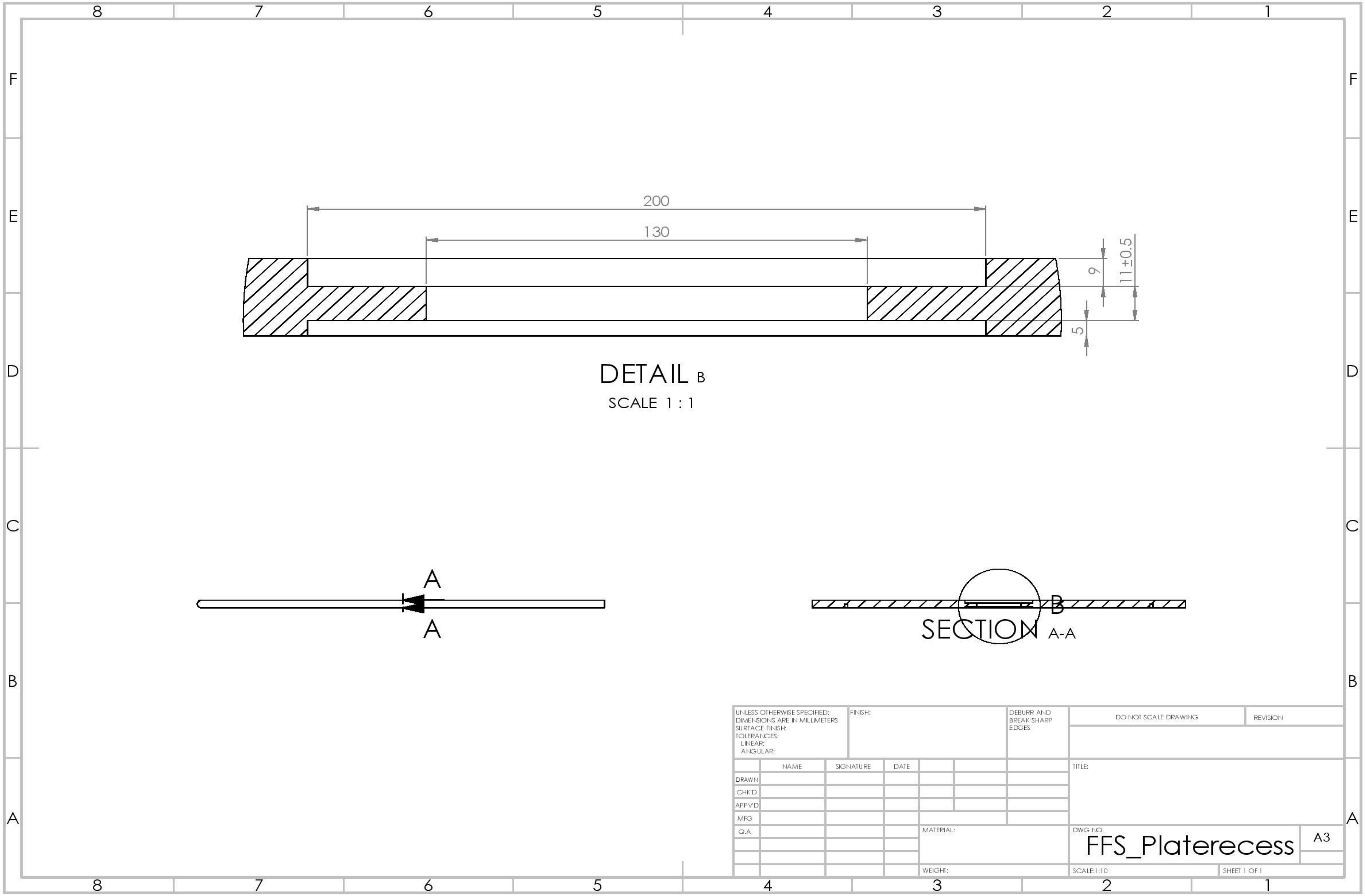
200
130
9
11±0.5
5
DETAIL B
SCALE 1 : 1
A
A
B
SECTION A-A
UNLESS OTHERWISE SPECIFIED:
DIMENSIONS ARE IN MILLIMETERS
SURFACE FINISH:
TOLERANCES:
LINEAR:
ANGULAR:
FINISH:
DEBURR AND BREAK SHARP EDGES
DO NOT SCALE DRAWING
REVISION
NAME
SIGNATURE
DATE
DRAWN
CHK'D
APPV'D
MFG
Q.A
TITLE:
MATERIAL:
DWG NO.
FFS_Platerecess
A3
WEIGHT:
SCALE:1:10
SHEET 1 OF 1

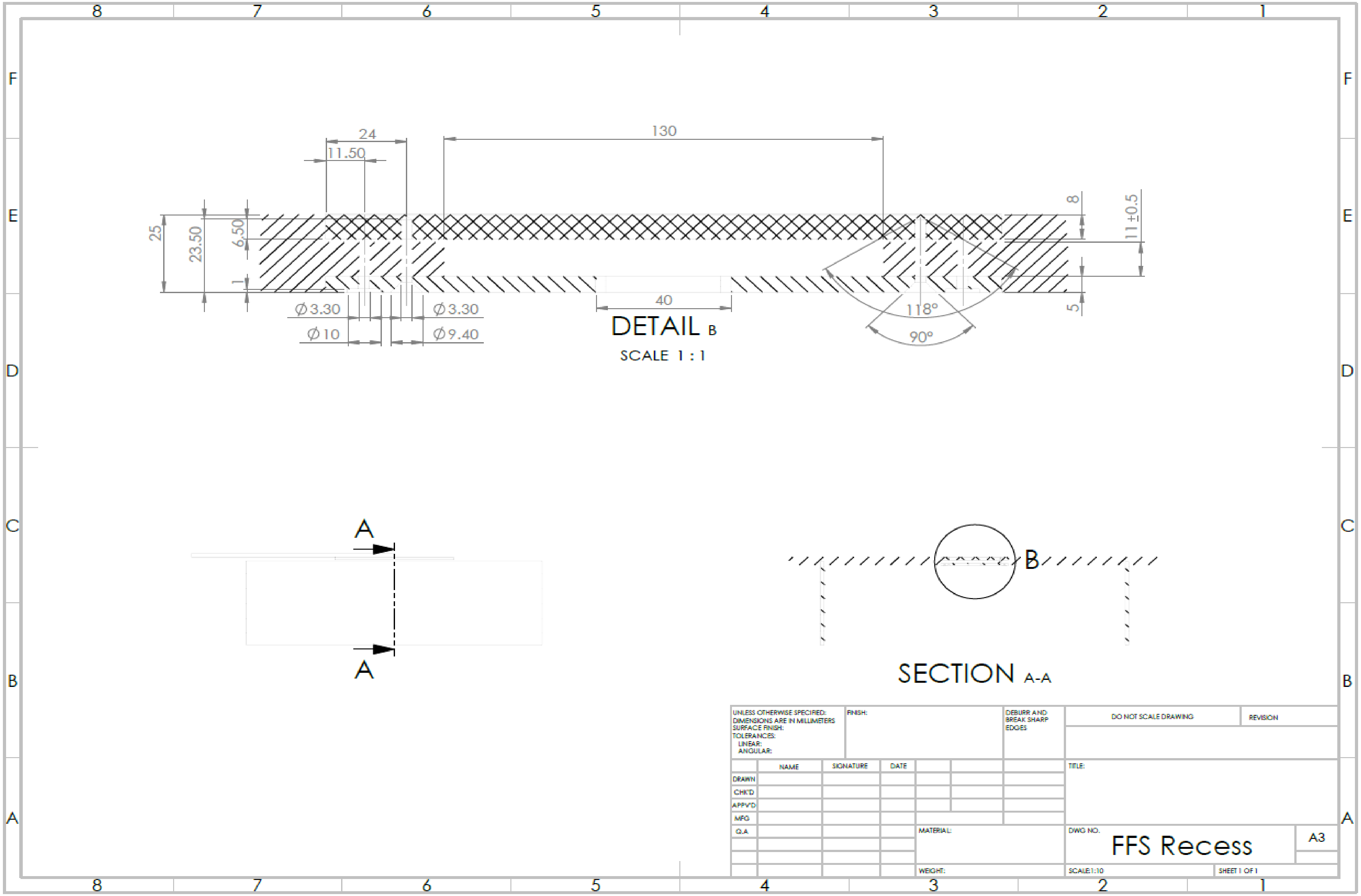
24
11.50
130
25
23.50
6.50
1
8
11 ±0.5
5
Ø3.30
Ø10
Ø3.30
Ø9.40
40
118°
90°
DETAIL B
SCALE 1 : 1
A
A
B
SECTION A-A
UNLESS OTHERWISE SPECIFIED:
DIMENSIONS ARE IN MILLIMETERS
SURFACE FINISH:
TOLERANCES:
LINEAR:
ANGULAR:
FINISH:
DEBURR AND BREAK SHARP EDGES
DO NOT SCALE DRAWING
REVISION
NAME
SIGNATURE
DATE
DRAWN
CHK'D
APPV'D
MFG
Q.A
TITLE:
MATERIAL:
DWG NO.
FFS Recess
A3
WEIGHT:
SCALE:1:10
SHEET 1 OF 1

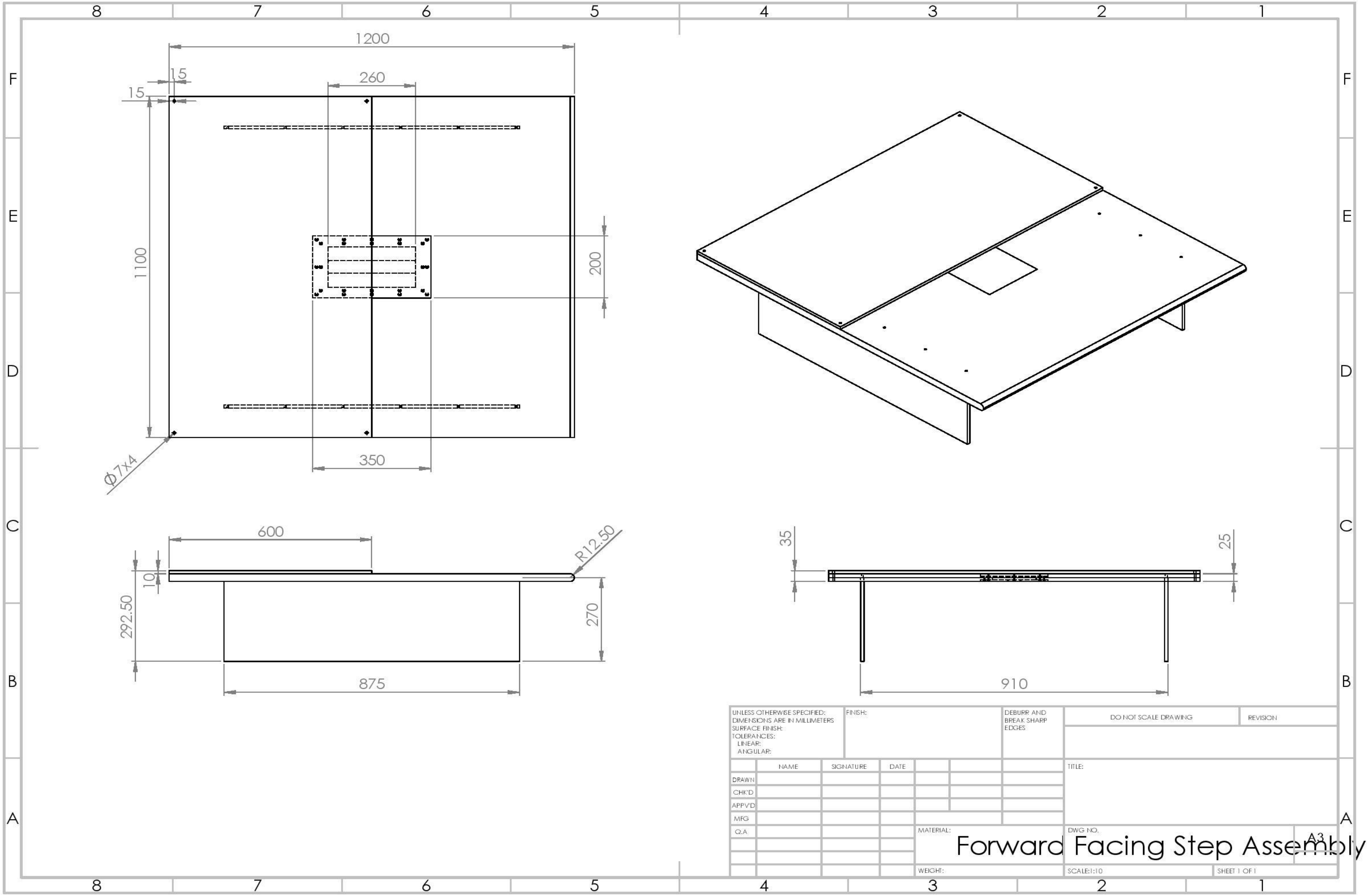
1200
15
15
260
1100
200
350
Ø7x4
600
R12.50
10
292.50
270
875
35
25
910
UNLESS OTHERWISE SPECIFIED:
DIMENSIONS ARE IN MILLIMETERS
SURFACE FINISH:
TOLERANCES:
LINEAR:
ANGULAR:
FINISH:
DEBURR AND BREAK SHARP EDGES
DO NOT SCALE DRAWING
REVISION
NAME
SIGNATURE
DATE
DRAWN
CHK'D
APPV'D
MFG
Q.A
TITLE:
MATERIAL:
DWG NO.
Forward Facing Step Assembly
A3
WEIGHT:
SCALE:1:10
SHEET 1 OF 1

5. Experimental Methodology

5.1 Particle Image Velocimetry Image Evaluation Technique

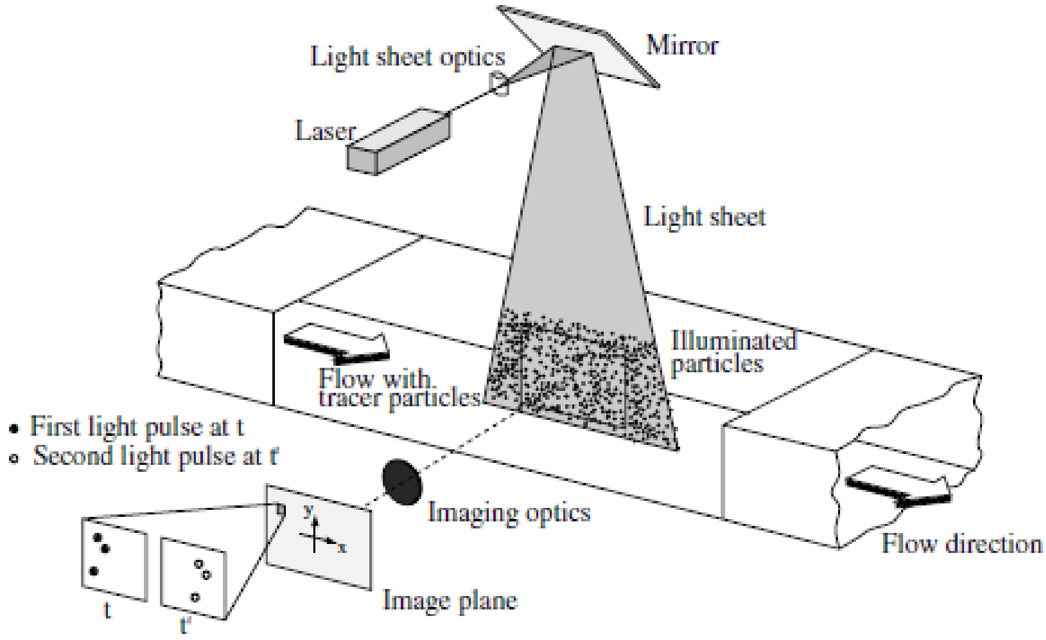

Figure (7): General Particle Image Velocimetry Setup [10], (Kompenhans et al., 2007, Fig. 1.4)

The light sheet projecting through the flow field lights up the tracer particles released from downstream. The particles are illuminated in a stroboscopic fashion such that no streaks are produced when the camera is taking pictures of the flow field. The camera takes a picture of the state of the flow field after each laser pulse. Given that the only information available to decipher is the laser pulse separation time and the displacement of the particle, a particle velocity is able to be obtained. The resultant velocity is a straight line approximation since information of the flow behaviour between each pulse is lost. The lack of continuity means that the curvature or acceleration of the particles in the flow file are not possible to be retained. Though increasing the frequency of the laser pulses and the sampling rate of the signals reduces the margin for error and better describes the state of the fluid within the flow. Trouble can arise from sheet lighting being used to illuminate the droplets passing through in spite of studying the flow field in a planar direction. The reason emanates from the fact that this PIV technique cannot account for 3D effects taking places. For instance if a particle recorded in an initial laser pulse may potentially dive outside of the illuminating sheet light in the interval before the next signal arrives. Therefore a loss pair means that a small segment of the velocity vector cannot be analysed. There is also potential difficulty in correlating individual particles because of the homogeneity of the tracer particles [9] (Kompenhans et al., 2007, pg132). Instead of tracking the flow analytically, the velocity vectors are obtained through WIDIM (Window Image Deformation Iterative Multigrid). The interrogation window analysing the particles is reduces in size and is gradually shifted plane wise. A cross-correlation method is then used to account for changes and deformations in the flow pattern and the velocities are re-interpolated using a finer grid refinement to more accurately determine the flow pattern.

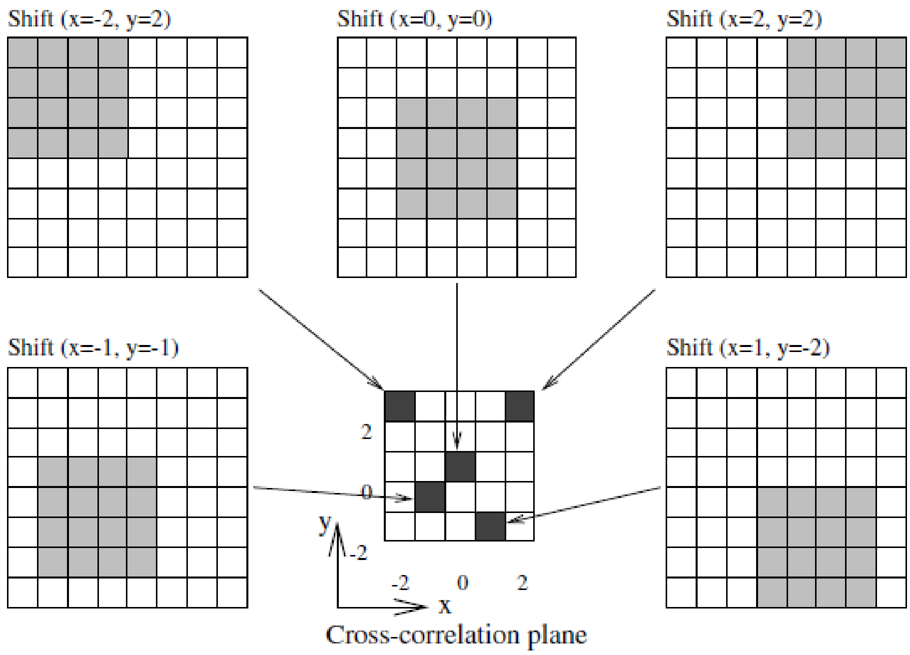

Figure (8): Multigrid Cross Correlation example, 4x4 grid template shifted along and 8x8 pixel sample in which direct cross correlation to produce a 5x5 pixel correlation [10], (Kompenhans et al., 2007, Fig. 5.12)

5.2 Experimental Arrangement

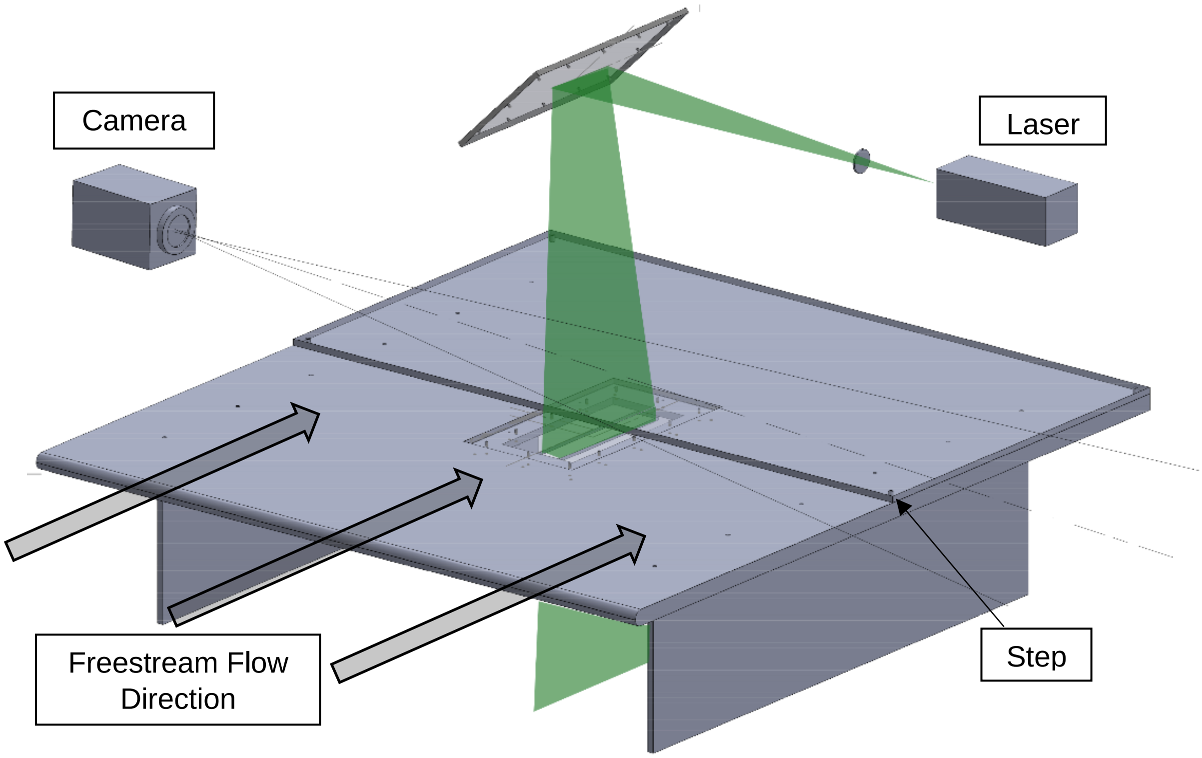

Figure (9): PIV setup for Forward Facing Step

Testing is conducted in City University's Aeronautical Laboratory in the T2 Low Speed Wind Tunnel. The dimensions of the test section are 1.2 m × 0.8 m × 2 m (W × H × L). Figure (9) illustrates the arrangement in which PIV measurements are taken during wind tunnel testing. Prior to taking results, a preliminary control test is performed without the step attached to the model. This eliminates systematic errors during the experiment and so that the various parameters are documented under the conditions of the room at the time of testing. Particle image velocimetry is used to determine the thickness of the boundary layer for a given Reynolds number. After the preliminary control tests are conducted, the large Perspex step is screwed back into the wooden plate, and testing is allowed to commence. The Perspex step height is 10mm and the front of the step is situated 600mm downstream from the leading edge.

Firstly, the wind tunnel is set to operate under the chosen parameters. A steady airflow of 20m/s must be established prior to commencing the process of recording data. Olive oil droplets are diffused upstream through a Laskin nozzle and the droplets act as the medium in which the light is illuminating the position of particles in the airflow. The Nd:YLF high-speed laser (Litron LDY300) is used to illuminate the particles and operates at a frequency of 1kHz at a wavelength of 527nm. The laser is projected through an optic, converting it into sheet light which is directed at a mirror pointing into the viewing window which is dissecting the flow field at the step. The viewing window is made out of Perspex and allows the laser to penetrate through the model. A high speed camera (Phantom M310) recording the movements of the flow field frame by frame. Synchronisation of the signals between the camera and the laser is provided by a software called TSI Insight 4G to reliably capture the position of the particles at each interval. The camera tracks the instantaneous velocity field of the flow through each light pulse which particles in a series of pictures at a high frequency.

Two fields of view will be recorded, one studying the region in front of the step (FOV1) and the other will be studying the rear of the step (FOV2). The size of the FOV is 26 x 17.3 mm^2 and the resolution of the picture taken is 1280x800. The laser pulse separation in front of the step of the laser is 15 μs while the rear of the step is 10 μs. The camera is to be synchronised accordingly. Since the camera is positioned a considerable distance from the experimental apparatus, a long range microscope is used to focus in the area of interest, thus providing enough detail to be captured which is required for analysis. Data is collected from the instantaneous velocity field for different ratios of δ/h and values of Re_h.

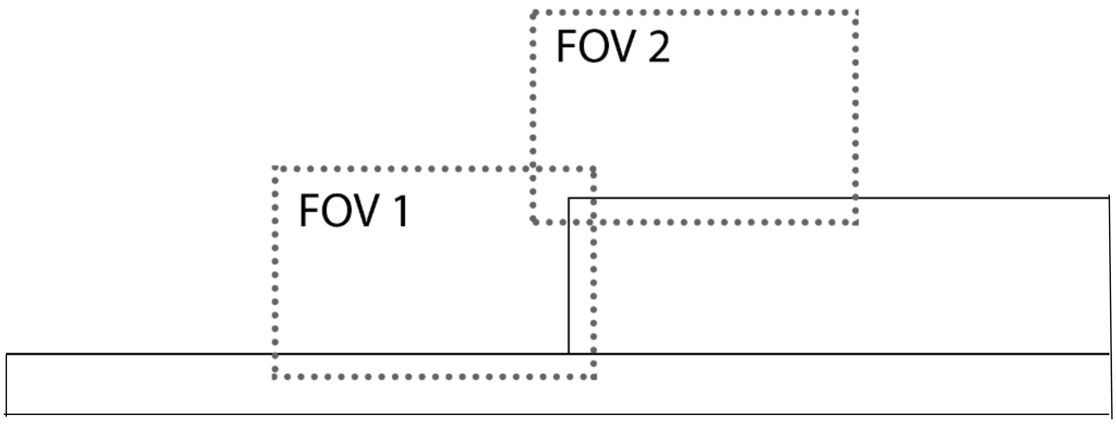

Figure (10): Camera Positioning of Experimental Setup

Vast quantities of data are gathered since high frequency laser subsequently means that immense numbers of raw pictures are taken and are require processing to determine vector field of instantaneous flow.

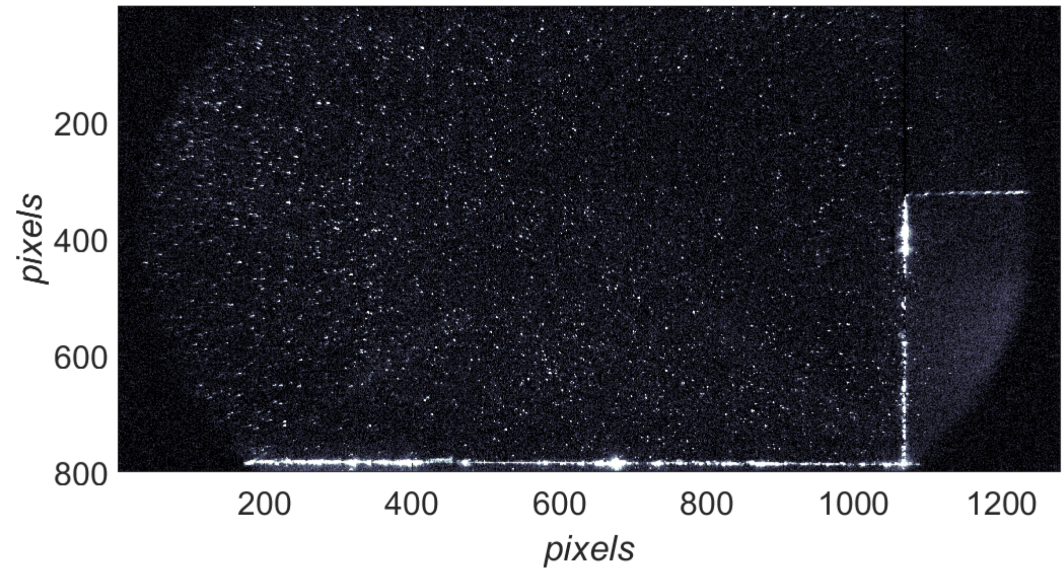

Figure (11): Front of Step Raw Photograph (FOV1)

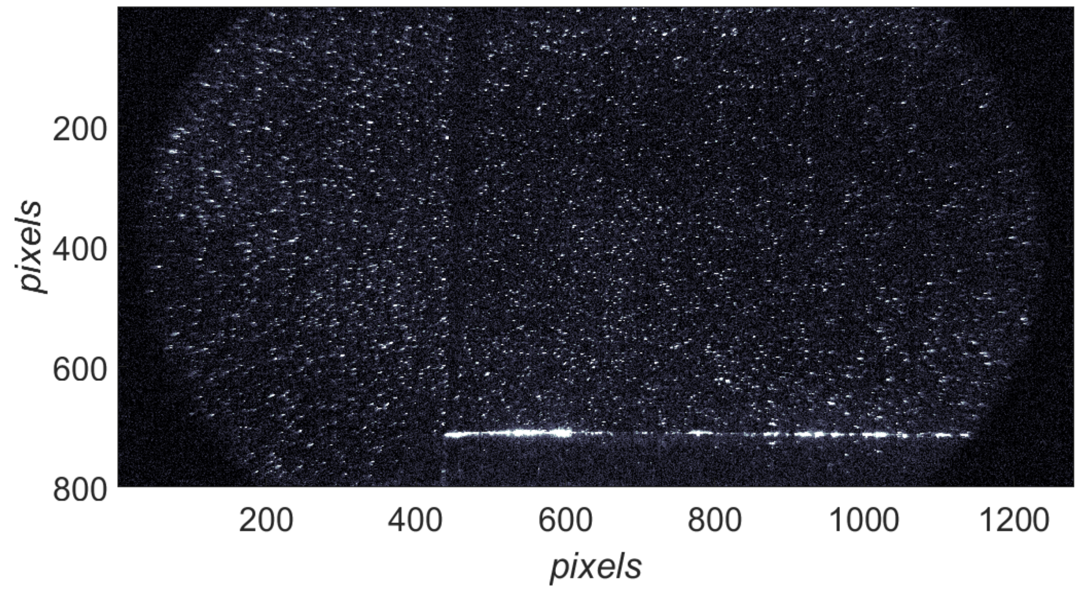

Figure (12): Top (Rear) of Step Raw Photograph (FOV2)

PIVLab is a GUI developed using the MATLAB software to process the raw footage. This program establish the vector field using image correlation. The individual particle movements in each time interval are used to determine the entire instantaneous velocity field for a specific point in time. Finally MATLAB scripts are written to post-process the results so as to observe the different characteristics of the flow field. The vector field is spread over a mesh correlating to the coordinate system determined by the pixels on the photographs observed in the flow field. The images from the different fields of view are meshed together to observe the flow field as the vectors exit out of plane. Various data is graphed such as the time average movement of the velocity field, the RMS of the instantaneous flow, the turbulence intensity and additionally the vorticity of generated by the step.

Parameter	Quantity	
Flow Speed U_∞	20 m/s	
FOV Area	26 x 17.3 mm^2	
Magnification Factor	1.08	
Particle Diameter d_p	~ 1μm	
Laser Pulse Separation dt	15 μs (Front FOV)	10 μs (Rear FOV)
Particle Displacement in Freestream	~15 pixel (Front FOV)	~ 10 pixel (Rear FOV)
Ensemble size N	1000	
Final interrogation window	24 x 24 pixels	
Vector Spacing 0.25mm	0.25 mm	

Table (2): PIV Laser/Camera and Image Evaluation Configuration

6. Results and Discussion

6.1. Instantaneous Vector Field

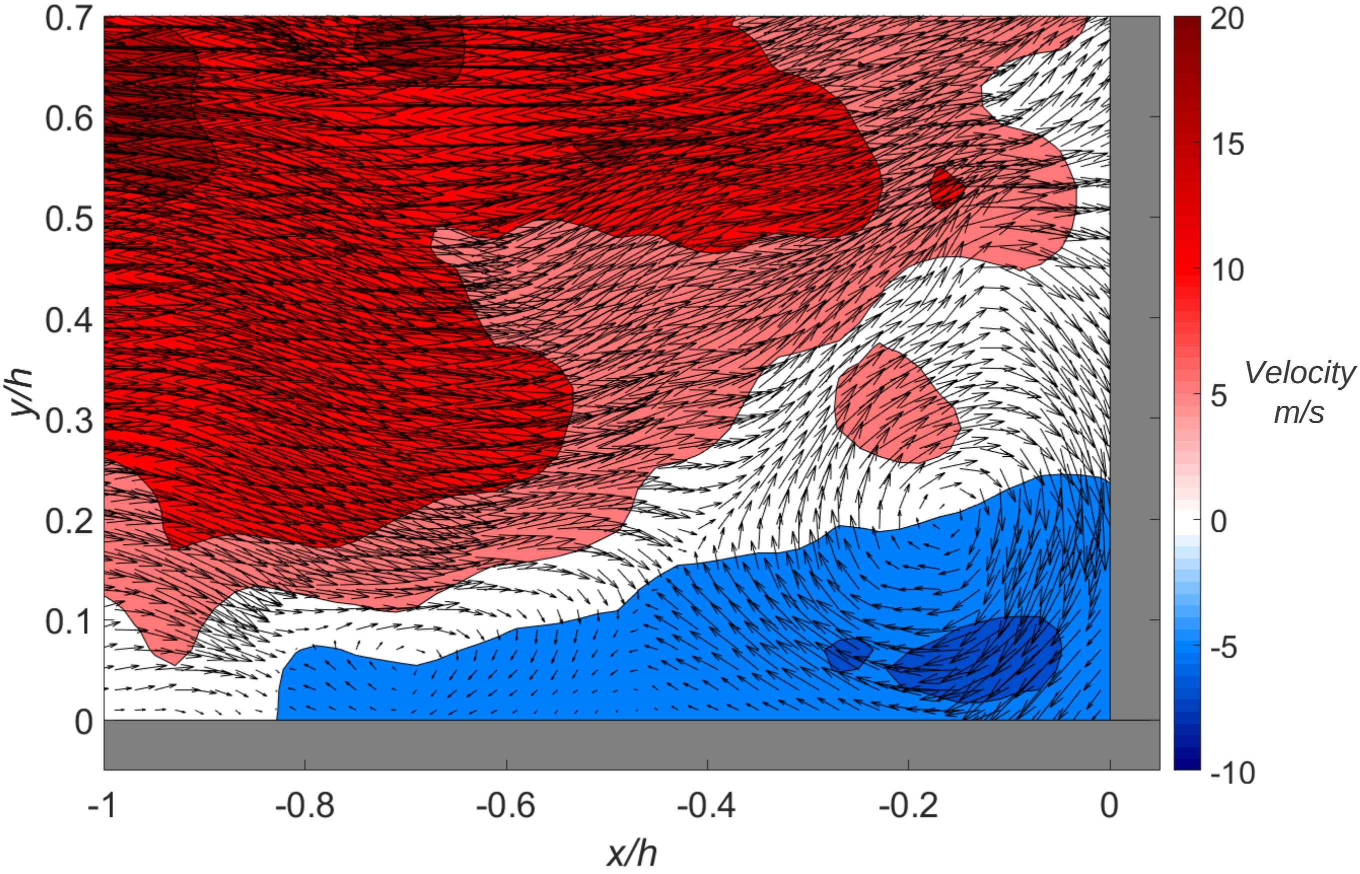

Figure (13): Instantaneous Vector Field of Separation Region in Front of Step

Figure (13) highlights the movement of the flow within the separation region at the Front of the Step. The recirculation region appears to be split into two segments which rotate clockwise under the influence of the motion of the oncoming flow toward the step. The core of the smaller recirculating segment of flow appears at x/h=-0.7 which is relatively close to the location of the flow separation. The separation bubble appears to be somewhat cumulative as a result of being situated near the wall of the step; this promotes more vertical growth of the bubble. As the flow approaches closer to the step, the effect of the adverse pressure gradient becomes more prominent, helping escalate the size of the separation bubble. The larger of the 2 recirculating regions occurs closer to the face of the step at x/h=-0.2 where the flow diverges more so from the surface, thus providing more space for larger vortical structures emerge. The height the bubble eventually peaks at y/h=0.6.

The freestream to flow over the separated region while the separation region is circulates around itself. The freestream appears to provide a minor contribution feeding into the separation bubble in the region of -0.6 < x/h < -0.4. However for the most part there appears to be very limited interaction between the outer flow of the freestream and the separated region. The recirculation region seems to be self-contained and explains why the separation bubble doesn't see further growth through the duration of the experiment. The nature of the recirculation means that the upper region moves in the direction of freestream but a lower magnitude of velocity whilst the direction of the flow is reversed along the floor as indicated by the blue region. The core and middle of the recirculating region appears to be fairly stagnant whilst the outward layers of flow appear to have more velocity because of the influence of the freestream on the separated region. At y/h=0.6, the flow appears to reattach itself to the face of the step because the growth potential of the separation region is limited, therefore the boundary layer flowing over the separation bubble has the opportunity allowing itself to reattach itself to the wall.

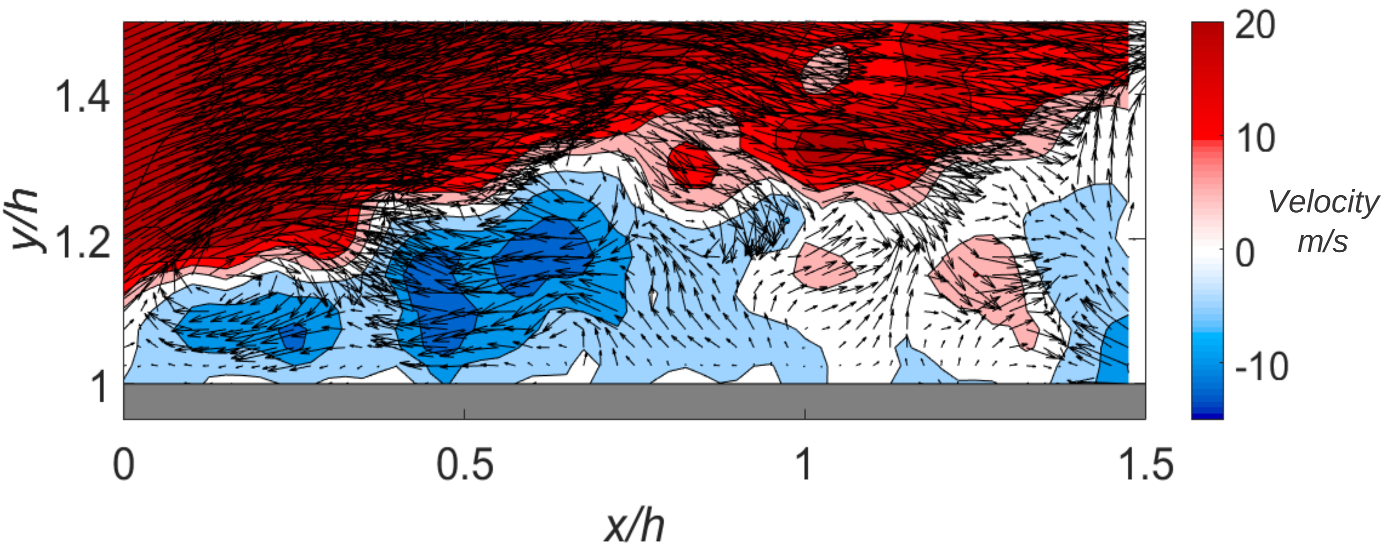

Figure (14): Instantaneous Vector Field of Separation Region on Top of Step

Figure (14) illustrates the motion of the flow within the separation region atop of the step. The flow appears to be more chaotic in comparison to the flow at the front of the step, this likely due to the instabilities generated as the flow approached the step. Additionally, separation occurs immediately after leaving the tip of the step because the flow is unable to turn a sharp corner at high velocity. The chaotic nature of the flow atop of the step is also resultant of the development of a shear layer which divides the recirculation region and the flow in the freestream. Initially the shear layer appears to be rather thin immediately after separation. However it can be seen that the shear layer appears to thicken progressively downstream as a result. The unstable boundary layer becomes increasingly turbulent as the flow extends downstream. The turbulent shear layer is the driving force of the motion within the recirculation region and the strength of it dictates the speed of recirculation and the vorticity within the separated region. The bubble has a core that has a high velocity magnitude and the outer layers of the separation region are weaker as they have large radius in which the flow is cycling unlike the inner layers of the separation region. Moreover the outer layers of the recirculation are more subject to friction from the surface of the step and that from the adjacent recirculating layers which result in a slower movement of flow. Resultantly the velocity is stronger at the core of the recirculation.

Unlike the separation bubble in Figure (13) which has high cumulative potential with regards to the strong adverse pressure gradient generated by the step, the separation atop of the step appears to be a lot more elongated. The separation bubble on top of the step only reaches a height of 0.3 y/h at most which is half that of the front of the step. Although the bubble has a much higher aspect ratio as a result of a greater horizontal flow velocity. Furthermore, since the separation atop of the step is more unstable and chaotic than the initial separation, the flow is therefore more likely to be subject to the inertial force of the freestream velocity giving rise to a longer separation length downstream. The speed of the flow is higher over the top surface, this means that the boundary layer will travel further over a shorter time period.

6.2. Mean Velocity Contours

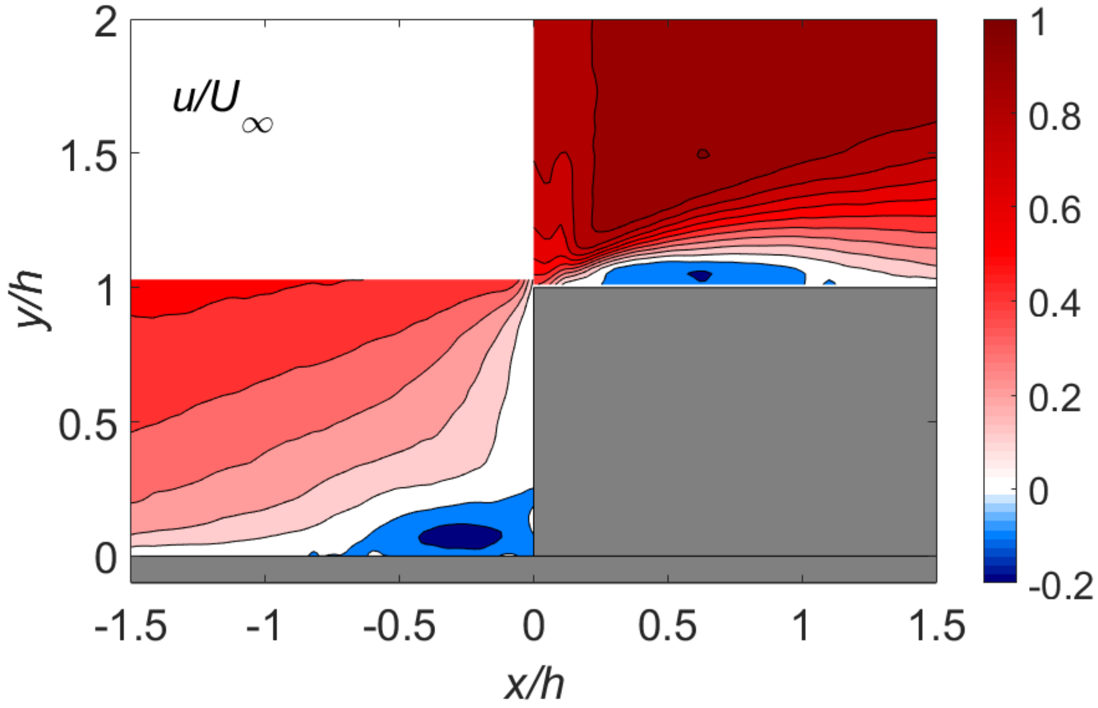

Figure (15): Horizontal Mean Velocity Contour

Figure (15) illustrates the dimensionless horizontal mean velocity contour across the entire configuration of the Forward Facing Step. The diagram gives an overview of the general characteristics of the flow behaviour when confronted with a step. The scenario highlights the two recirculation regions that emerge as a result of flow separation. Flow velocity within the recirculation region is 5 to 10 times slower in comparison to the freestream velocity and is therefore fairly stagnant with this region. The effects of the adverse pressure gradient are also visible from the diagram in Figure (15). In front of the step, the first four red layers flowing over the separation bubble are significantly slower on average which could be an indicator deceleration in the flow as a result of boundary layer having to flow over separation bubble. Furthermore having the oncoming flow encountering the face of the step would cause even further stagnation. Once the flow separates from the tip of the step the effects of the adverse pressure gradient are relinquished slightly as there is a more rapid restoration to the fluid velocity. The separation region over the top of the step is not as tall as the initial bubble and results in a weaker adverse pressure gradient and therefore the flow subsequently is able to carry higher horizontal mean velocity.

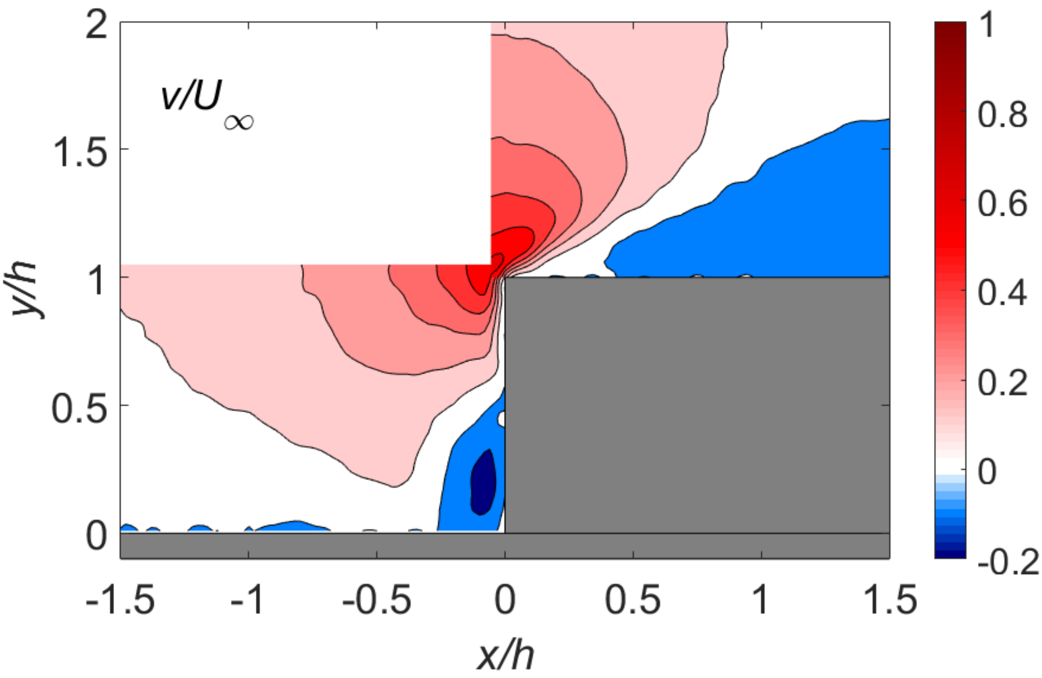

Figure (16): Vertical Mean Velocity Contour

Figure (16) depicts the dimensionless vertical mean velocity helping characterise the other aspects which are not visible on the horizontal velocity contours. For instance the reattachment of the flow on the face of the step is more clearly visible on the Figure (16) at the location y/h=0.6. Upwash appears to be prevalent after reattaching to the face of the step and the vertical component reaches its peak after leaving the tip of the step which could be as a result pressure building up from beneath from flow being forced upwards. But once the flow leaves the tip of the step, the effect of the freestream becomes immediately apparent and skews the vertical component of the velocity and forces the flow to proceed horizontally. However, downstream it can be seen that there is massive region where the average vertical component of the flow is moving downwards. The rationale behind this occurrence is because the separation bubble doesn't grow downstream. As shown in Figure (15), the bubble has an elliptical shape and eventually tends towards reattachment after extending downwards by at least 1 step height. As the boundary flows over the separation bubble, the velocity profile will on average flow downwards whilst tending towards reattachment towards the surface. Additionally, the mixing within the shear layer drags in layers of fluid from the freestream which could contribute towards the overall trend of the downward movement of the flow. The observation effect of the upper separation bubble can be seen in Figure (15) and (16) and is creating distortion in the flow field which change the direction of the streamlines as shown in the horizontal contours and also the massive depression which extends downstream whilst managing to even affect the freestream flow.

Figures (15) and (16) also demonstrate the dominant fluid motions which arise at different locations of the Forward Facing Step. This is particularly visible at the recirculation regions whereby the fluid flow is highly varied. In figure (15) the horizontal contours appear mainly along the floor next to the step indicating a predominantly horizontal motion opposite to the freestream flow. But the horizontal velocity contours do not extend vertically along the face of the step since the flow is not permeating through the step, it is stagnating. However it can be seen in Figure (16) whereby there is a higher density of vertical velocity contours along the face of the step indicating that the flow is moving downwards from the face of the step. Although the vertical velocity contours are less spread across the floor near the step which indicates horizontal motion taking effect as the flow is recirculating.

6.3. Turbulent Properties of Flow Field

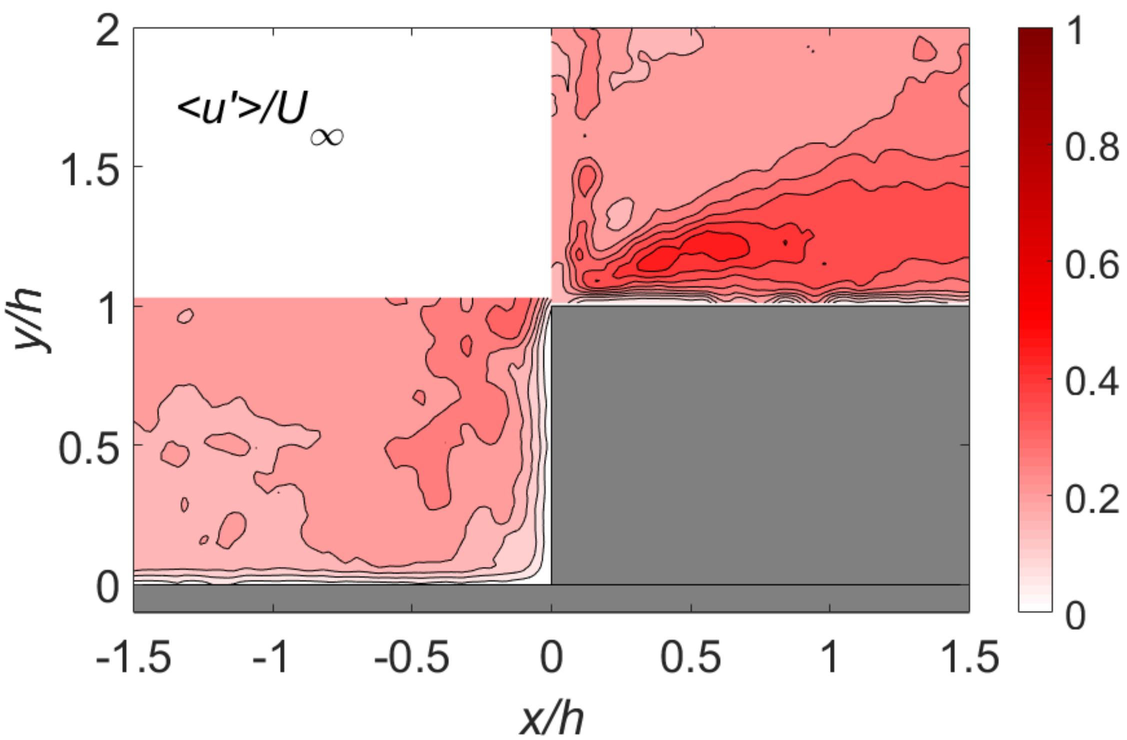

Figure (17): Instantaneous Horizontal RMS Velocity Contour

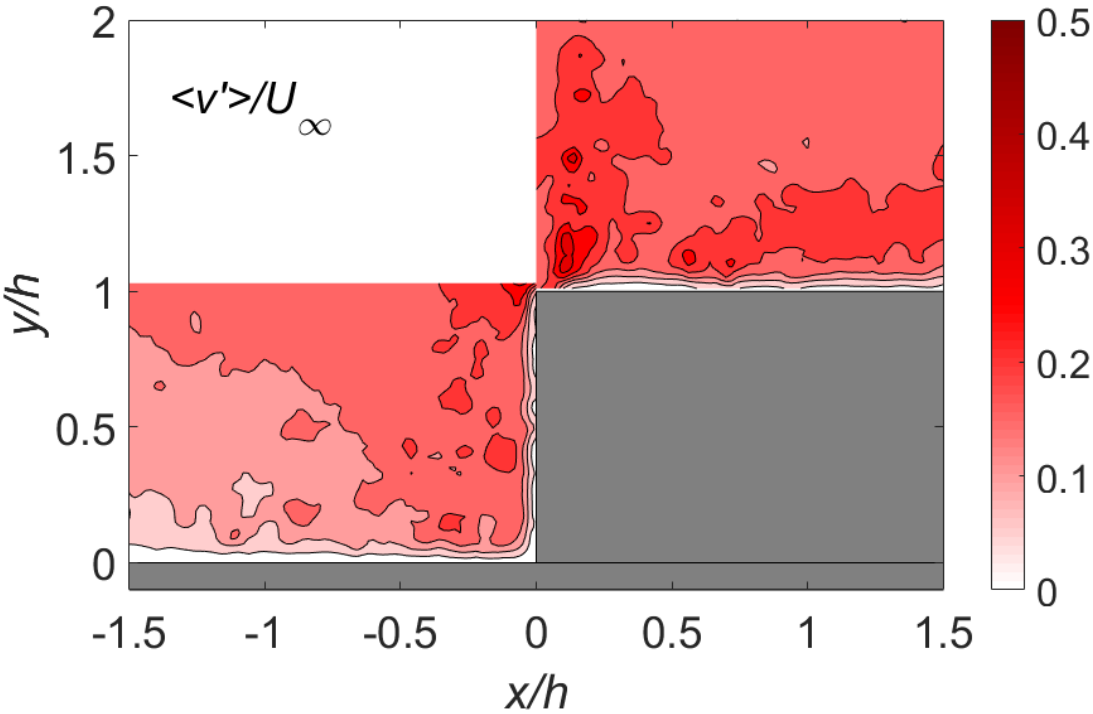

Figure (18): Instantaneous Vertical RMS Velocity Contour

Figures (17) and (18) show the components of the RMS velocity contours of the instantaneous flow over the Forward Facing Step highlighting the unsteady nature of the flow. Both components indicate higher fluctuations in the flow downstream compared to the upstream segment. The peaks of the streamwise component ⟨u'⟩ follow the contours of the shear layer as the flow extends downstream. Likewise, this is true for the ⟨v'⟩ component, however it sees an overall weaker average in comparison to the streamwise component since the inertia of the freestream is dominating and dictating the overall direction of the flow. Although the wall normal component gets stronger as it extends downstream as the flow returns on approaching the step for reattachment. The separation regions see little to no fluctuations in the RMS values seeing as the recirculating flow is independent of the freestream. The RMS along the walls in the separation regions are zero and along the shear layer a non-zero value is observed due to the effect of the shear layer driving the recirculating flow at a relatively constant rate.

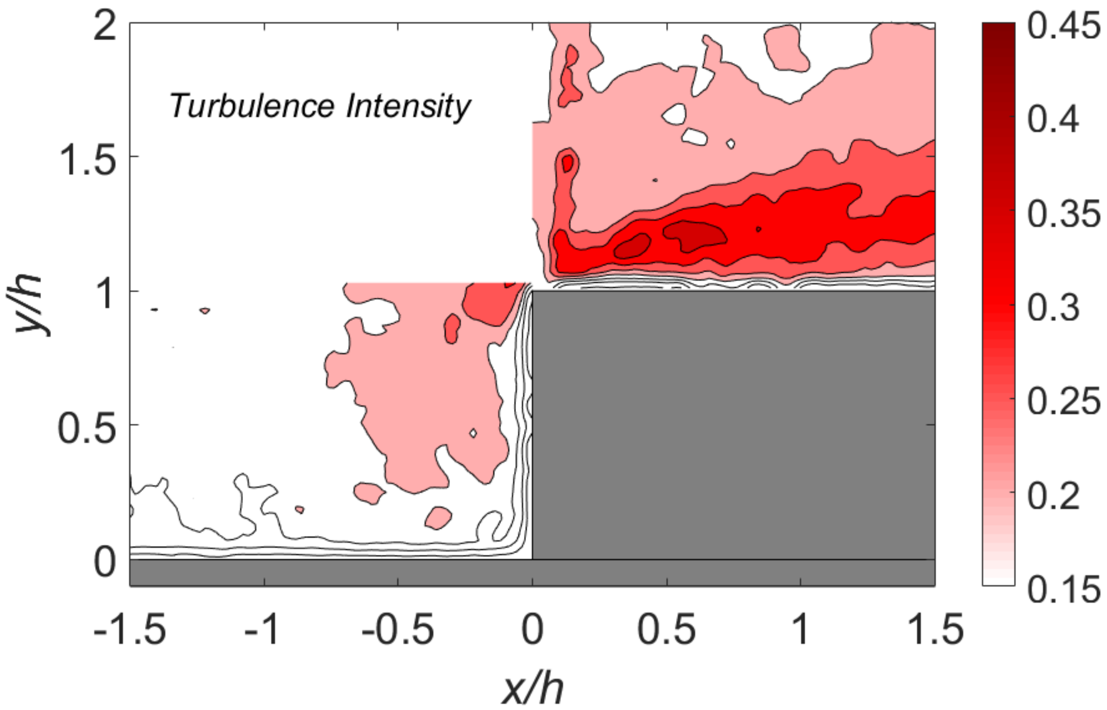

Figure (19): Turbulence Intensity of flow over FFS

Figure (19) shows the variation in turbulence as the flow passes over the step. The turbulent levels are less than 0.15, which is very low prior to approaching the step. This supports the previous observations of the flow seen upstream of the step whereby the fluctuations are minimal. However the closer the boundary layer approaches to the step, the stronger the effect of the adverse pressure becomes. Once the initial separation occurs fore of the step, the boundary layer becomes more unstable and thus slightly increases the turbulence intensity. Although the flow doesn't see a full transition at this location. Downstream of the tip of the step it can be seen that there is a dramatically higher turbulence intensity. The turbulence intensity increases 3-fold downstream of the step as a result of a variety of factors. The adverse pressure gradient generated by the separation region atop of the step is a source of resistance toward the already unsteady boundary layer. Furthermore the shear layer has a significant contribution in the generation of turbulence downstream since the flow is mixing significantly and in addition pulling flow in from the freestream. The majority of the turbulence emanates from the shear layers which has the most unstable segments of airflow; the regions outside the shear layer see a significantly reduced level in turbulence intensity. In the separation regions there is little to no turbulent activity since the average velocity of the flow within the separation region is significantly less compared to the freestream velocity. Therefore there little or no turbulence or vortical structures emerging in the separation regions.

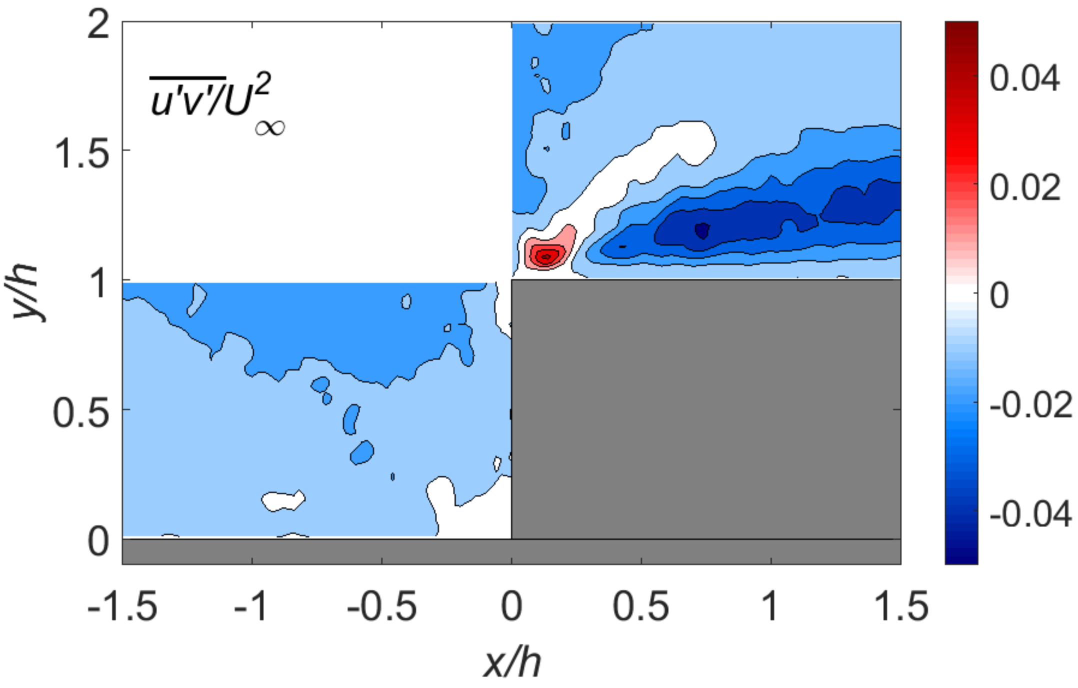

Figure (20): Reynolds Stresses over the Forward Facing Step

Figure (20) illustrates the variation in Reynolds Stresses which are incurred as a result of the fluctuating velocity components and the unsteady nature of viscous flow. The peaks of the Reynolds shear stresses highlight where the turbulence is most prominent. The Reynolds stresses are fairly well aligned with each other in comparison to the turbulence intensity shown in Figure (20). The negative peaks generally occur over the top of the step as a result of the strong shear layer interacting with the flow in the freestream. As a result strong vortical activity is detected which extends in the downstream segment of the flow.

6.4. Mean Vorticity Plot

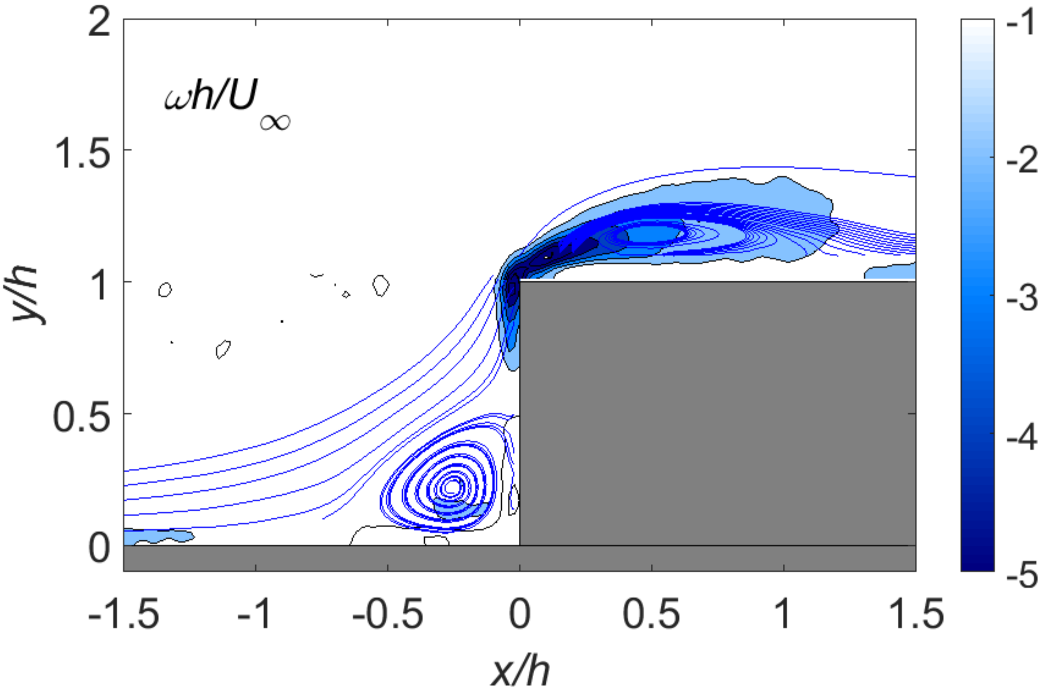

Figure (21): Mean Vorticity Contours Over Forward Facing Step

Figure (21) shows the mean vorticity of the flow approaching the Forward Facing Step. Vorticity is calculated using the curl of the vector field to give the rotationality of specific points across the field. Upstream flow has very low vorticity because of the low turbulence intensity induced upon the flow. There is some light rotational elements along the wall of the step as a result of shearing force generated in a viscous flow. The vorticity of the flow is approximately 5 times greater downstream compared to the upstream value as a result of the turbulent transition over the step. The shear layer has a significant effect in vortex generation. It is especially apparent since the region very close to the top surface of the step has an extremely low vorticity by contrast. The contrast highlights the independence of the recirculation region from the shear flow and the flow in the free stream. After 1 step height downstream of the step, the vorticity appears to reduce and stabilise itself as a due to the favourable pressure gradient re-energising the boundary layer to promote reattachment to the surface of the step. The shear layer effect dissipates downstream after the reattachment as hinted by the reduced vorticity downstream, and thusly there is less turbulence.

7. Conclusion

Achievements and Highlights

The project has observed the qualitative aspects of flow separation emerging from a flow approaching a stepped geometry. The effect of the adverse pressure gradient on the boundary layer induces the flow separation mechanism, giving rise to the emergence of a pair of separation regions. Visualisations of the separated regions show that the recirculating flow is independent of the outside freestream flow. Furthermore, an unsteady shear layer develops downstream over the top of the step in which the flow significantly transitions from laminar to turbulent because of the mixing of layers and the velocity gradient within the shear layer. The unsteady nature of the shear layer creates fluctuations in the flow field which creates undulations in the flow downstream. The fluctuating flow downstream is great source of turbulent activity and shear stress in addition to the significant vorticity generated when triggered by the boundary layer separation off the tip of the step.

However, it wasn't possible to quantitatively investigate the reattachment lengths of the separation bubbles because of significant project delays and time constraints on approach to the deadline. The objective to experimentally analyse the flow separation was undermined by delays to the project. In addition, there is very little data published on the separation length (Xs) of the foremost separation bubble, therefore it's difficult to draw conclusions of the separation bubble growth without additional data being collected. The inability to conduct the experiment within the time constraints meant that the physical boundaries and limitations cannot be identified and thusly could not validate results against the non-dimensional data from historical experiments.

Progress to Plan

Numerous problems arose in the duration of the project as a result, in particular the inability to fit a time slot to complete the manufacturing modification of the Forward Facing Step. The completion of the design work overran by approximately a month because numerous iterations of the design were reviewed and changes were made over the course of the month. Applying the changes from the suggested improvements took a considerable amount of time. After having completing the final draft of the design, the drawings were submitted to the manufacturing department at the end of December. However, the workshop was occupied with other projects which were prioritised over the Forward Facing step. A technician was finally assigned to the project in mid-February so the limitations of the design could be discussed. Following his suggestions, further changes were made to the drawings to make the manufacturing process easier so the resources and time could be used more effectively. For instance selecting a standardised thickness of Perspex for the viewing window so the technician wouldn't have to spend time reducing the thickness and refinishing the surface to make it transparent. The order for the materials needed for the modification ran late into March since the relevant staff were absent and the available technicians were heavily burdened with several other projects deep into March/April. The materials arrived in early April, however the Easter Break arrived and all the staff went on leave. The manufacturing could only commence after the deadline for the project. I could not conduct my own experiment to investigate how the separation lengths change according to variations in step height and Reynolds number.

The contingency plan put into action was to post-process a collection of raw PIV images recorded in a previous experiment. The scale of the model used in the previous experiment intrinsically has a very small width to height ratio which could give rise to 3D effects and could be disruptive to the illuminated airflow. Though the recorded data could still be used to qualitatively characterise the behaviour of a flow over a stepped geometry.

The intention in the future is to finish the intended experiment to independently investigate the flow separation using different δ/h ratios and different Reynolds numbers. Furthermore the results will be validated against the statistical data collected from previous experimental data to see how the results fit within the distribution.

Learning Outcomes

The intention of the module is to learn how to plan and execute an engineering project effectively. There are many gaps in knowledge that must be covered with regards to this aerodynamic application. Reading many scientific papers and textbooks on the various subjects becomes more efficient over time especially when the subject knowledge increases. Extracting the relevant material from the literature speed up as the search requirements for particular information become more stringent. This was especially true when scouring for previous FFS data. From the information gathered a clearer picture emerges; the objective and the intention of the project becomes more apparent. Furthermore the research allowed me to select reasonable step heights to incorporate into the design such that δ/h could be easily compared and validated against the published results of previous experiments. After finding the statistical correlation of changing various parameters such as the δ/h ratio or the Re, it inspired the desired outcome of the project. The motivation shifted to not only to study the qualitative aspects of the flow, but also to draw some statistical conclusions.

In the realms of design and manufacturing, despite the inherent problems that occurred in the duration of the project. The difficulties of attempting to insert myself into the schedules of other workers became apparent. However, it provided an insight on the communication lines between different people involved in the project. In terms of arranging meetings to discuss plans, exchange ideas and also to describe ones desires in an engineering context to provide other with the understanding of the importance behind the motivation of certain elements of a design.

Overall the project has created a huge impression on me in terms of solving challenges behind the design of the Forward Facing Step which has required a certain level of creativity and assertiveness to accomplish the goal. The culmination of various schools of knowledge in aerodynamics are condensed and provide a good background behind the flow behaviour. The principles how to integrate the knowledge into a coherent analysis of a flow over stepped geometry.

Metrics

Engineering projects are very complicated and very demanding, thusly requiring a lot of preparation. Therefore it is becomes apparent that initiative and assertiveness are necessary to complete tasks as early as possible. This is especially true when there are tasks that are dependent upon others, the progress is limited by the capacity of a person's ability to cater to your desire e.g. the manufacturing of the FFS. When future planned activities are pinned to the critical activity, progress cannot be made on the subsequent tasks of the project. As a result the entire is pushed behind schedule. So it is advisable to provide the most lee-way possible in the case of unforeseeable events future which could hinder progress.

As the accumulation of information and knowledge increases, the understanding of the subject area becomes clearer. There are suddenly more goal orientated motives to pursue behind the various tasks you have already planned for yourself. It will also provide you design constraints. For instance the research of the Forward Facing Step papers led to the inspiration of the step height size selection. Additionally the reattachment lengths inspired the dimensions of the length of the viewing window. Having a broad understanding of the project helps communicate the design intentions with clarity to other engineers and technicians such that there is no confusion. This will allow goals to be met without corners being cut.

8. Glossary

AVG – Adverse Pressure Gradient

DNS – Direct Numerical Simulation

FFS – Forward Facing Step

FOV – Field of View

GUI – Graphical User Interface

Nd:YLF – Neodymium-doped yttrium lithium fluoride

PIV – Particle Image Velocimetry

RMS – Root Mean Square

TBL – Turbulent Boundary Layer

WIDIM – Window Image Deformation Iterative Multigrid

δ – Boundary Layer Thickness

dt – Time Interval

d_p – Particle diameter

h – Step Height

W – Width

X_L – Reattachment Length (x/h) (Aft Recirculation Region)

X_S – Separation Length (x/h) (Fore Recirculation Region)

Re – Reynolds Number

ω – Vorticity

9. Appendix

9.1 Tables

For tables (3) and (4) the $X_L\delta/h$ values were all with respect to y for calculation for linear regression. Reh and h/δ were both were in relation to x.

Calculating Linear Regression for Reh against XLδ/h										
Sx	Sy	Sxx	Syy	Sxy	a	b	xbar	ybar	n	r
960240	138.0	90010206400	1265.1	7742221	2.95	5.4E-05	33111.72	4.76	29	0.53

Table (3): *Linear Regression Calculation for Reynolds number against normalised separation length*

Calculating Linear Regression for h against XLδ/h										
Sx	Sy	Sxx	Syy	Sxy	a	b	xbar	ybar	n	r
43.0	138.0	127	1265.1	377.8	0.69	2.74	1.48	4.76	29	0.88

Table (4): *Linear Regression Calculation for step height against normalised separation length*

Sxx,Syy,Sxy for Re_h			Sxx,Syy,Sxy for Step Height		
(Sxx)	Syy)	(Sxy)	(Sxx)	(Syy)	(Sxy)
41990400	276.1	107667.6923	59.17	276.1	127.8
829440000	136.1	336000	11.11	136.1	38.9
16435240000	277.8	2136666.667	11.11	277.8	55.6
11236000000	105.6	1089223.058	6.28	105.6	25.8
45369000000	110.8	2242105.263	6.28	110.8	26.4
729000000	61.0	210937.5	4.34	61.0	16.3
19360000	16.0	17600	4.00	16.0	8.0
691690000	36.0	157800	4.00	36.0	12.0
671846400	30.6	143293.5849	3.56	30.6	10.4
2500000000	45.1	335714.2857	2.04	45.1	9.6
2500000000	51.0	357142.8571	2.04	51.0	10.2
0	33.0	0	2.04	33.0	8.2
289000000	20.9	77714.28571	2.04	20.9	6.5
707560000	18.0	112791.5194	1.39	18.0	5.0
2830240000	20.0	238115.4299	1.39	20.0	5.3
2560000	3.6	3026.047565	1.28	3.6	2.1
4000000	1.5	2444.444444	1.23	1.5	1.4
44089600	2.8	11043.65904	1.08	2.8	1.7
176890000	11.1	44241.16424	1.08	11.1	3.5
420250000	2.4	31441.71779	0.38	2.4	0.9
10240000	0.9	3082.105263	0.28	0.9	0.5
0	1.6	0	0.26	1.6	0.7
441000000	1.6	26250	0.17	1.6	0.5
400000000	1.0	20000	0.06	1.0	0.3
23040000	0.2	2307.692308	0.05	0.2	0.1
77440000	0.1	2640	0.04	0.1	0.1
691690000	0.2	11046	0.04	0.2	0.1
2500000000	0.1	13461.53846	0.04	0.1	0.1
368640000	0.2	8464.516129	0.01	0.2	0.0

Table (5): *Calculating Sxx, Syy, Sxy for Re_h and h/* δ parameters in relation to X_L

9.2 Sample MATLAB Post Processing Scripts

9.21 Processing Instantaneous Flow Data

```
%% Read Vector Field

imax = 107;
jmax = 67;

istart = 18; iend = 92;
jstart = 6; jend = 66;

%Referencing File Location
fileroot = 'F:\step\V20_front_01run\PLT_WS24\';

nfile=200;

for ifile =1:nfile

    filename = [fileroot 'B',num2str(ifile,'%.5d'),'.plt'];

    flowdata = importdata(filename);

    x = flowdata.data(:,1);
    y = flowdata.data(:,2);
    u = flowdata.data(:,3);
    v = flowdata.data(:,4);

    x = reshape(x,imax,jmax);
    y = reshape(y,imax,jmax);
    u = reshape(u,imax,jmax);
    v = reshape(v,imax,jmax);

    x = x(istart:iend,jstart:jend);
    y = y(istart:iend,jstart:jend);
    u = u(istart:iend,jstart:jend);
    v = v(istart:iend,jstart:jend);

end


 %Plotting Instantaneous Flow Field
    crange = [-5:2:20];
    G=contourf(x,y,-u,crange);
    colormap bluewhitered
    ha=gca;
    set(ha,'xdir','reverse')
    colorbar;hold on;
    axis equal;
    quiver(x,y,u,v,3,'k');

 %I manually saved the variables
```

9.22 Processing Instantaneous RMS Flow Data

```
%% Load Meanflow
imax = 107; jmax = 67;

filename = 'F:\step\Mean\Step_V20_Front_N1000_WS24.plt';
flowdata = importdata([filename]);

x = flowdata.data(:,1);
y = flowdata.data(:,2);
u = flowdata.data(:,3);
v = flowdata.data(:,4);

umean=u;
vmean=v;

x = reshape(x,imax,jmax);
y = reshape(y,imax,jmax);
umean = reshape(umean,imax,jmax);
vmean = reshape(vmean,imax,jmax);

%% Plot the contour of the airfoil
folder = 'F:\step\V20_front_01run\PLT_WS24\';

nfile = 200;

urms = 0;
vrms = 0;
uv = 0;

for ifile = 1:nfile

    filename = [folder 'B0' num2str(ifile,'%.4d'),'.plt'];

    flowdata = importdata(filename);

    u = flowdata.data(:,3);
    v = flowdata.data(:,4);

    u = reshape(u,imax,jmax);
    v = reshape(v,imax,jmax);

    urms = urms + (u - umean).^2;
    vrms = vrms + (v - vmean).^2;

    uv = uv+(u - umean).*(v - vmean);

end

urms = sqrt(urms/nfile);
vrms = sqrt(vrms/nfile);
uv = uv/nfile;

savematrix = [x(:) y(:) umean(:) vmean(:) urms(:) vrms(:) uv(:)];
save ('FrontRMS2.0.mat','x','y','u','v','umean','vmean','uv','urms','vrms')
contourf(x,y,vrms,[0:1:10]);
colormap bluewhitered
```

9.23 Merging Mean Velocity Contours

```
%Front Part of Step

%Defining Experimental Conditions

h = 460;
pixel = 0.0217;          %step height/pixel
U0 = 20;                 %Free Stream Velocity
dt = 15e-6;              %FOV 1 Laser Pulse Separation
Vrange = [-1:0.1:1.0];   %Velocity Range

%Loading Variables
load('F:\step\Filip_Script\Variables1.1\MeanFront.mat'); % x y u v

%Non-Dimensionalising Wall Distance
x= (-x/h)+0.449;
y= (y/h)-0.03;

%Non-Dimensionalising Velocity Components
u = -u*pixel/1000/dt/U0;
v = v*pixel/1000/dt/U0;

%Creating Mesh as domain for inserting interpolated velocity
[xi yi] = meshgrid(-1.92:0.02:-0.02,0.01:0.02:1.05);

%Interpolating for velocities to plot over mesh
ui = interp2(x',y',u',xi,yi);
vi = interp2(x',y',v',xi,yi);

%Plotting Contour of Front of Step
contourf(xi+0.02,yi-0.02,ui,Vrange,'linewidth',0.5);%
hold on;
colormap bluewhitered
hold on;

%%
%Aft/Rear of Step

h = 460;                   %step height in pixels
U0 = 20;                   %Free Stream Velocity
dt = 10e-6;                %FOV 2 Laser Pulse Separation

load('F:\step\Filip_Script\Variables1.1\MeanRear.mat'); % x y u v

x= -x/h+1.93;              %Dimensionless x-Coordinates (x/h)
y= y/h+0.889;              %Dimensionless y-Coordinates (y/h)

u = -u*pixel/1000/dt/U0;   %Dimensionless u-velocity u/U
v = v*pixel/1000/dt/U0;    %Dimensionless v-velocity v/U

%Creating Mesh as domain for inserting interpolated velocity
[xi yi] = meshgrid(0:0.02:1.98,1.1:0.02:2.24);
```

```
%Interpolating for velocities to plot over mesh
ui = interp2(x',y',u',xi,yi);
vi = interp2(x',y',v',xi,yi);

contourf(xi,yi-0.0889,ui,Vrange,'linewidth',0.5);
colormap bluewhitered
hold on;


%%
%Dimensionless Velocity Range
caxis([-0.2 1.0])
colorbar;
%%
%
axis equal;
axis([-1.5,1.5,-0.1,2]); %axis limits
colormap bluewhitered
%%
% Plot Step

rectangle('Position',[0 0 2 1],'FaceColor',[0.5 0.5 0.5]);
rectangle('Position',[-2 -0.1 4 0.1],'FaceColor',[0.5 0.5 0.5]);

%%
%Formatting Graph

xlabel('\itx/h');
ylabel('\ity/h');

text(-1.4,1.7,' {\itu/U_{\infty}}','FontSize',26);
set(gca,'FontSize',26);
set(gcf,'Position',[100 0 1200 600]);
```

9.24 Merging Instantaneous RMS Flow Data

```
%Front Part of Step

%Defining Experimental Condtions

h = 460;
pixel = 0.0217;          %step height/pixel
U0 = 20;                 %Free Stream Velocity
dt = 15e-6;              %FOV 1 Laser Pulse Separation
Vrange = [0:0.05:1];     %Velocity Range

%Loading Variables
load('F:\step\Filip_Script2.0\Variables2.0\FrontRMS2.0.mat'); % x y u v

%Non-Dimensionalising Wall Distance
x= (-x/h)+0.449;
y= (y/h)-0.03;

%Non-Dimensionalising Velocity Components
u = -u*pixel/1000/dt/U0;
v = v*pixel/1000/dt/U0;

urms = urms*pixel/1000/dt/U0;
vrms = vrms*pixel/1000/dt/U0;

%Creating Mesh as domain for inserting interpolated velocity
[xi yi] = meshgrid(-1.92:0.02:-0.02,0.01:0.02:1.05);

%Interpolating for velocities to plot over mesh
ui = interp2(x',y',urms',xi,yi);
vi = interp2(x',y',vrms',xi,yi);

%Plotting Contour of Front of Step
contourf(xi+0.02,yi-0.02,ui,Vrange,'linewidth',0.5);%
hold on;
colormap bluewhitered
hold on;

%%
%Aft/Rear of Step

h = 460;                   %step height in pixels
U0 = 20;                   %Free Stream Velocity
dt = 10e-6;                %FOV 2 Laser Pulse Separation

load('F:\step\Filip_Script2.0\Variables2.0\RearRMS2.0.mat'); % x y u v

x= -x/h+1.93;                    %Dimensionless x-Coordinates (x/h)
y= y/h+0.889;                   %Dimensionless y-Coordinates (y/h)

u = -u*pixel/1000/dt/U0;   %Dimensionless u-velocity u/U
v = v*pixel/1000/dt/U0;    %Dimensionless v-velocity v/U

urms = urms*pixel/1000/dt/U0;
vrms = vrms*pixel/1000/dt/U0;
```

```
%Creating Mesh as domain for inserting interpolated velocity
[xi yi] = meshgrid(0:0.02:1.73,1.1:0.02:2.24);


%Interpolating for velocities to plot over mesh
ui = interp2(x',y',urms',xi,yi);
vi = interp2(x',y',vrms',xi,yi);

contourf(xi,yi-0.0889,ui,Vrange,'linewidth',0.5);
% colormap bluewhitered
hold on;


%%
%Dimensionless Velocity Range
caxis([0 1.0])
colorbar;
%%
%
axis equal;
axis([-1.5,1.5,-0.1,2]); %axis limits
% colormap bluewhitered
%%
% Plot Step

rectangle('Position',[0 0 2 1],'FaceColor',[0.5 0.5 0.5]);
rectangle('Position',[-2 -0.1 4 0.1],'FaceColor',[0.5 0.5 0.5]);

%%
%Formatting Graph

xlabel('\itx/h');
ylabel('\ity/h');

text(-1.4,1.7,' {\it<u''>/U_{\infty}}','FontSize',26);
set(gca,'FontSize',26);
set(gcf,'Position',[100 0 1200 600]);
```

9.25 Merging and Plotting Vorticity

```
%Front Part of Step

%Defining Experimental Condtions

h = 460;
pixel = 0.0217;          %step height/pixel
U0 = 20;                 %Free Stream Velocity
dt = 15e-6;              %FOV 1 Laser Pulse Separation


%Loading Variables
load('F:\step\Filip_Script2.0\Variables2.0\FrontRMS2.0.mat'); % x y u v

%Non-Dimensionalising Wall Distance
x= (-x/h)+0.449;
y= (y/h)-0.03;

%Non-Dimensionalising Velocity Components
u = -u*pixel/1000/dt/U0;
v = v*pixel/1000/dt/U0;

urms = urms*pixel/1000/dt/U0;
vrms = vrms*pixel/1000/dt/U0;

umean = -umean*pixel/1000/dt/U0;
vmean = vmean*pixel/1000/dt/U0;

%Creating Mesh as domain for inserting interpolated velocity
[xi yi] = meshgrid(-1.92:0.02:-0.02,0.01:0.02:1.05);

%Interpolating for velocities to plot over mesh
ui = interp2(x',y',umean',xi,yi);
vi = interp2(x',y',vmean',xi,yi);
vorticity = curl(xi,yi,ui,vi);

%Plotting Contour of Front of Step
contourf(xi+0.02,yi-0.02,vorticity,[-6:1],'linewidth',0.5);%
hold on;
colormap winter
hold on;

%Adding Flow Streamlines
xstart = [-1.8 -1.8 -1.8 -1.8 -1.8 -0.75];
ystart = [0.05 0.1 0.15 0.2 0.25 0.1];
streamline(xi,yi,ui,vi,xstart,ystart);
xstart = -0.25*ones(5,1);
ystart = [0.05 0.1 0.15 0.2 0.25];
streamline(xi,yi,ui,vi,xstart,ystart);

%%
%Aft/Rear of Step

h = 460;                   %step height in pixels
U0 = 20;                   %Free Stream Velocity
dt = 10e-6;                %FOV 2 Laser Pulse Separation
```

```
load('F:\step\Filip_Script2.0\Variables2.0\RearRMS2.0.mat'); % x y u v

x= -x/h+1.93;                    %Dimensionless x-Coordinates (x/h)
y= y/h+0.889;                   %Dimensionless y-Coordinates (y/h)

u = -u*pixel/1000/dt/U0;   %Dimensionless u-velocity u/U
v = v*pixel/1000/dt/U0;    %Dimensionless v-velocity v/U

urms = urms*pixel/1000/dt/U0;
vrms = vrms*pixel/1000/dt/U0;
umean = -umean*pixel/1000/dt/U0;
vmean = vmean*pixel/1000/dt/U0;

%Creating Mesh as domain for inserting interpolated velocity
[xi yi] = meshgrid(0:0.02:1.73,1.1:0.02:2.24);

%Interpolating for velocities to plot over mesh
ui = interp2(x',y',umean',xi,yi);
vi = interp2(x',y',vmean',xi,yi);
vorticity = curl(xi,yi,ui,vi);

contourf(xi-0.1,yi-0.0889,vorticity,[-6:-1],'linewidth',0.5);

%Adding Flow Streamlines
xstart = 0*ones(3,1);
ystart = [1.005 1.01 1.1];
streamline(xi,yi,ui,vi,xstart,ystart);

xstart = 0.15*ones(9,1);
ystart = [1.11:0.005:1.15];
streamline(xi,yi,ui,vi,xstart,ystart);

xstart = 0.2*ones(9,1);
ystart = [1.11:0.005:1.15];
streamline(xi,yi,ui,vi,xstart,ystart);
%  colormap winter
hold on;

%Dimensionless Velocity Range
caxis([-5 -1])
colorbar;
%%
%
axis equal;
axis([-1.5,1.5,-0.1,2]); %axis limits
 colormap bluewhitered

% Plot Step
rectangle('Position',[0 0 2 1],'FaceColor',[0.5 0.5 0.5]);
rectangle('Position',[-2 -0.1 4 0.1],'FaceColor',[0.5 0.5 0.5]);

%Formatting Graph
xlabel('\itx/h');
ylabel('\ity/h');

text(-1.4,1.7,' {\it\omegah/U_{\infty}}','FontSize',26);
set(gca,'FontSize',26);
set(gcf,'Position',[100 0 1200 600]);
```

9.3 Project Timeline

Figure (22): Gantt chart of planned activities prior to commencing project

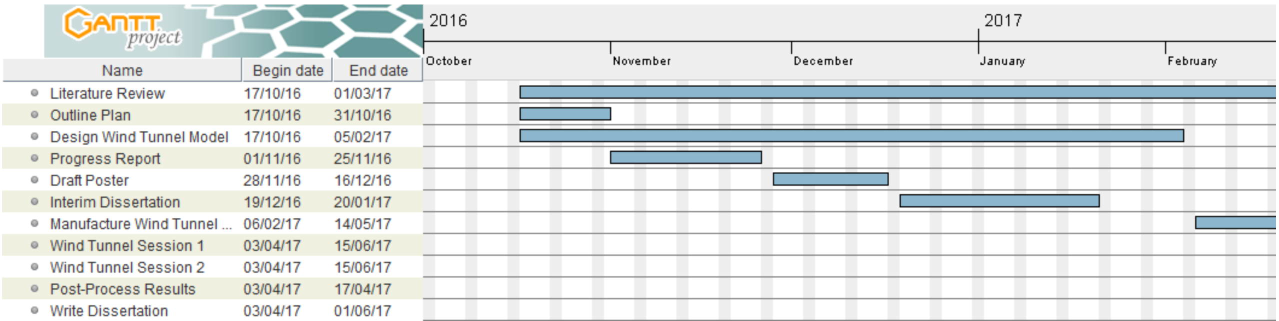

Figure (23a): Actual progress of activities during project

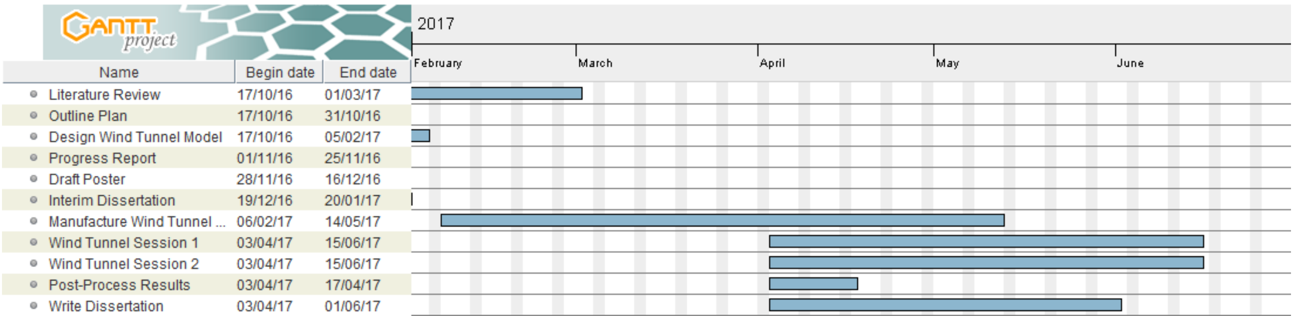

Figure (23b): Actual progress of activities during project

10. References

E. Fiorentini et al. Velocity and wall pressure correlations over a forward facing step. Physics of fluids. [1]

Available at: http://www.aivela.org/Fiorentini_paper19.pdf

Date Accessed: 07/11/16

M. J. Sherry et al. (2009) Flow Separation Characterisation of a Forward Facing Step Immersed In a Turbulent Boundary Layer. [2]

Available at:

http://people.eng.unimelb.edu.au/imarusic/publications/Conferences/Sherry_TSFP_2009.pdf

Date Accessed: 08/11/16

Z. Sun, Experimental Investigation on the Flow Separations at a Forward-Facing Step. [3]

Available at: http://openaccess.city.ac.uk/15671/3/AAC_Step.pdf

Date Accessed: 09/11/16

D S Pearson et al. (2011) Investigation of turbulent separation in a forward-facing step forward [4]

Available at: http://iopscience.iop.org/article/10.1088/1742-6596/318/2/022031/pdf

Date Accessed: 01/12/16

Awasthi, M, (2012) High Reynolds Number Turbulent Boundary Layer Flow over Small Forward Facing Steps [5]

Available at: https://theses.lib.vt.edu/theses/available/etd-06292012-120614/unrestricted/Awasthi_M_T_2012_2.pdf

Date Accessed: 01/12/16

Weijie Shao,(2014), Experimental Study of Turbulent Boundary Layer Flows Over Forward Facing Steps with Different Surface Conditions [6]

Available at: https://ir.library.dc-uoit.ca/bitstream/10155/463/1/Weijie_Shao.pdf

Date Accessed: 01/12/16

Syed Imran SHAH, Vortical Structures in Wall-Bounded Turbulent Flow with Recirculation [7]

Available at: http://iopscience.iop.org/article/10.1088/1742-6596/318/2/022022/pdf

Date Accessed: 01/12/16

Minsuk Ji and Meng Wang, Surface pressure fluctuations on steps immersed in turbulent boundary layers J. Fluid Mech. (2012), vol. 712, pp. 471_504. C Cambridge University Press 2012 471 doi:10.1017/jfm.2012.433 [8]
Available at:
Date Accessed: 07/12/16

Minsuk Ji and Meng Wang, Aeroacoustics of Turbulent Boundary - Layer Flow over Small Step [9]
Available at: http://enu.kz/repository/2010/AIAA-2010-6.pdf
Date Accessed: 07/12/16

Kompenhans, J., Raffel, M., Wereley, S. and Willert, C. (2007). Particle image velocimetry. 2nd ed. Berlin [u.a.]: Springer. [10]

J Nogueira et al. Analysis and alternatives in two-dimensional multigrid particle image velocimetry methods: application of a dedicated weighting function and symmetric direct correlation [11]
Available at:
http://extras.springer.com/2004/978-3-540-21423-6/Summary/PUB_MADRID_200602_1.pdf
Date Accessed: 15/04/17

Thielicke, W. & Stamhuis, E.J. (2014). PIVlab – Towards User-friendly, Affordable and Accurate Digital Particle Image Velocimetry in MATLAB. Journal of Open Research Software 2(1):e30,
Available at: http://dx.doi.org/10.5334/jors.bl

Thielicke, W. & Stamhuis, E.J. (2014): PIVlab - Time-Resolved Digital Particle Image Velocimetry Tool for MATLAB (version: 1.41),
Available at: http://dx.doi.org/10.6084/m9.figshare.1092508

Thielicke, W. (2014): The Flapping Flight of Birds - Analysis and Application. Phd thesis, Rijksuniversiteit Groningen,
Available at: http://irs.ub.rug.nl/ppn/382783069

Garcia, D. (2011): A fast all-in-one method for automated post-processing of PIV data. Experiments in Fluids, Springer-Verlag, 2011, 50, 1247-1259